Received: 26 July 2023 | Revised: 21 December 2023 | Accepted: 19 February 2024

DOI: 10.1111/gbi.12592

gebiology WILEY

ORIGINAL ARTICLE

# Hydrogeological controls on microbial activity and habitability in the Precambrian continental crust

Min Song[1] | Oliver Warr[1] | Jon Telling[1] | Barbara Sherwood Lollar[1,2]

[1]Department of Earth Sciences, University of Toronto, Toronto, Ontario, Canada

[2]Institut de Physique du Globe de Paris (IPGP), Université Paris Cité, Paris, France

**Correspondence**
Barbara Sherwood Lollar, Department of Earth Sciences, University of Toronto, Toronto, ON, Canada.
Email: barbara.sherwoodlollar@utoronto.ca

**Present address**
Oliver Warr, Department of Earth and Environmental Sciences, University of Ottawa, Ottawa, Ontario, Canada
Jon Telling, School of Natural and Environmental Sciences, Newcastle University, Newcastle upon Tyne, UK

**Funding information**
Natural Sciences and Engineering Research Council of Canada; Nuclear Waste Management Organization (NWMO); Canadian Institute for Advanced Research

## Abstract

Earth's deep continental subsurface is a prime setting to study the limits of life's relationship with environmental conditions and habitability. In Precambrian crystalline rocks worldwide, deep ancient groundwaters in fracture networks are typically oligotrophic, highly saline, and locally inhabited by low-biomass communities in which chemolithotrophic microorganisms may dominate. Periodic opening of new fractures can lead to penetration of surface water and/or migration of fracture fluids, both of which may trigger changes in subsurface microbial composition and activity. These hydrogeological processes and their impacts on subsurface communities may play a significant role in global cycles of key elements in the crust. However, to date, considerable uncertainty remains on how subsurface microbial communities may respond to these changes in hydrogeochemical conditions. To address this uncertainty, the biogeochemistry of Thompson mine (Manitoba, Canada) was investigated. Compositional and isotopic analyses of fracture waters collected here at ~1 km below land surface revealed different extents of mixing between subsurface brine and (paleo)meteoric waters. To investigate the effects this mixing may have had on microbial communities, the Most Probable Number technique was applied to test community response for a total of 13 different metabolisms. The results showed that all fracture waters were dominated by viable heterotrophic microorganisms which can utilize organic materials associated with aerobic/facultative anaerobic processes, sulfate reduction, or fermentation. Where mixing between subsurface brines and (paleo)meteoric waters occurs, the communities demonstrate higher cell densities and increased viable functional potentials, compared to the most saline sample. This study therefore highlights the connection between hydrogeologic heterogeneity and the heterogeneity of subsurface ecosystems in the crystalline rocks, and suggests that hydrogeology can have a considerable impact on the scope and scale of subsurface microbial communities on Earth and potentially beyond.

KEYWORDS
deep biosphere, groundwater, habitability, heterotrophy, hydrogeology, microbial metabolism, Precambrian crust

## 1 | INTRODUCTION

Precambrian crystalline crust represents more than 70% of the continental surface area of the Earth (Goodwin, 1996). These crustal settings are typically tectonically quiescent and contain approximately 30% of the total groundwater inventory on Earth, principally held in fracture networks (Ferguson et al., 2021; Warr et al., 2018). In these global settings, water-rock reactions, in particular hydration reactions (e.g., serpentinization) and radiolysis, can produce large amounts of $H_2$, comparable to $H_2$ production in the oceanic crust (Sherwood Lollar et al., 2014; Warr et al., 2019). Abiotic $H_2$ and oxidants such as sulfate produced indirectly from radiolysis are among the most important energy sources capable of sustaining deep subsurface ecosystems over geological time (Bomberg et al., 2021; Li et al., 2016, 2022; Onstott et al., 2019). This deep subsurface continental biosphere has been estimated to account for approximately 30% of prokaryotic biomass (Magnabosco et al., 2018). Increasingly, the importance of understanding the hydrogeological context of this subsurface biome has gained attention, as hydrogeological conditions have significant impact on subsurface habitability. For instance, the relative contribution of microbial methane in samples was found to increase substantially at sites with higher degrees of paleometeoric water recharge at several mines in the Witwatersrand basin (Sherwood Lollar et al., 2006; Ward et al., 2004). In some of the Witwatersrand basin mines where mixing of older fracture water and paleometeoric waters existed, taxonomically and metabolically diverse microorganisms including methanogens, methanotrophs, sulfate reducers, and sulfur oxidizers that are coupled with denitrification are found to have developed syntrophic partnerships, so as to overcome thermodynamic barriers imposed by the environments in the deep subsurface (Lau et al., 2016). In the 2.5-km-deep Outokumpu drilling hole, Finland, diverse archaeal and bacterial communities varied with depth with cell densities decreased from $10^5$ to $10^3$ cells $mL^{-1}$ and were mainly controlled by geological and hydrogeological conditions (Kietäväinen et al., 2013; Nyyssönen et al., 2014). These studies and others demonstrate how interaction with the surface hydrosphere can provide a means to supply additional energy and nutrient sources into the deep subsurface, as meteoric water penetrates the crust, microorganisms (Westmeijer et al., 2022), and eukaryotes (e.g., nematodes; Borgonie et al., 2015, 2019) may colonize and adapt to subsurface environmental conditions. The interactions between subsurface life and hydrogeology may play an important role in global cycles of key elements H, S, C, and N in the crust (e.g., Hubalek et al., 2016; Lollar et al., 2019; National Academies of Sciences, 2022; Onstott et al., 2006; Sherwood Lollar et al., 2007).

In Earth's deep Precambrian basement, connection with the surface hydrosphere can be restricted by low porosity and permeability, as evidenced by studies conducted in places such as Kidd Creek of the Canadian Shield and Moab Khotsong mine of South Africa, where the mean residence times of the 2–3 km deep fracture waters are estimated to be up to 100 s of millions of years or older (Holland et al., 2013; Warr et al., 2018, 2022). In these and other hydrogeologically isolated systems, low-biomass subsurface microorganisms are highly dependent on energy sources predominantly provided by water-rock reactions (e.g., Bomberg et al., 2021; Li et al., 2016, 2022; Lin et al., 2006; Lollar et al., 2019; Nisson, Kieft, et al., 2023; Purkamo et al., 2016).

While Kidd Creek and Moab Khotsong represent end-members of the most ancient and isolated groundwaters identified to date, sites with younger residence times ranging from thousands to tens and hundreds of millions of years are more common (Borgonie et al., 2019; Kietäväinen et al., 2013, 2014; Lippmann et al., 2003; Sherwood Lollar et al., 2007). Fracturing can be induced by natural processes such as impact events (Grieve & Therriault, 2000), faults and shears (Paventi, 1995), and strain and deformation (Sleep & Zoback, 2007). It may also be induced by changes due to mine operations and drilling (Frape et al., 1984; Warr, Giunta, et al., 2021). Indeed, the major geochemical and isotopic signatures of subsurface fracture waters of Precambrian Shield indicate that at many sites around the world, subsurface groundwater systems exhibit different degrees of mixing between the deep ancient brine and water of (paleo)meteoric origin (Frape et al., 1984, 2014; Warr, Giunta, et al., 2021).

One of the challenges in obtaining a global picture of the subsurface systems is the heterogeneities of both the hydrogeological conditions and ecosystems of the continental subsurface. In addition, considerable uncertainty remains on how subsurface microbial communities may react to different hydrogeological conditions. This study focuses on naturally occurring fracture water at approximately 1 km below surface at Thompson mine (Manitoba) on the Canadian Precambrian Shield. A previous study showed that Thompson fracture waters have relatively active microbial communities by applying microcosm culturing and Most Probable Number (MPN) techniques (Telling et al., 2018). A relatively high microbial diversity was found at Thompson compared to Kidd Creek (Lollar et al., 2019), although $H_2$-driven metabolic activity was increasingly inhibited by elevated ionic strength of the groundwater samples (Telling et al., 2018). In contrast to Kidd Creek where significant production of abiotic hydrocarbons occurs (e.g., Sherwood Lollar et al., 2002; Warr, Young, et al., 2021), past studies suggested Thompson is one of the Shield sites with a substantial microbial methane component (estimated at 30%–50%; Sherwood Lollar et al., 1993). In addition, the dissolved acetate and dissolved organic carbon in fracture waters of a site adjacent to Thompson mine (Birchtree mine) are suggested to be derived from the disseminated carbon in metasedimentary host rocks, based on their similar ranges in $\delta^{13}C$ values, unlike acetate and formate identified at Kidd Creek that are suggested to be produced by radiolysis (Sherwood Lollar et al., 2021).

The present study builds upon previous work which focused on $H_2$-utilizing metabolisms (Telling et al., 2018), and further investigates other potential metabolic activity in the same series of natural fracture water samples from Thompson mine at ~1 km below land surface. The objectives of this study are to investigate the major types of planktonic microorganisms in the hydrogeologically heterogeneous fracture waters of Thompson and to investigate the relationships between hydrogeological conditions and subsurface microbial activity.

## 2 | MATERIALS AND METHODS

### 2.1 | Study site

Thompson mine is located in the Thompson Nickel Belt (TNB) area of northern Manitoba, Canada (55.72° N, 97.835° W; Figure 1). The TNB lies at the northwestern margin of the Superior Province of the Canadian Shield and adjoins the Trans-Hudson Orogen in Manitoba. The nickel deposits here are associated with ultramafic and metasedimentary rocks of the Paleoproterozoic Ospwagan group of the TNB (2.4–1.88 Ga), which deposited unconformably on the Archean basement rocks of the Superior Province (e.g., Lightfoot et al., 2017). Both the Ospwagan Group and the underlying Archean basement underwent multiple phases of deformation and intense metamorphism during the Hudsonian Orogeny (ca. 1.9–1.7 Ga) (Lightfoot et al., 2017). Most of the Ni-Cu sulfide deposits are hosted in the Pipe Formation of the Ospwagan group, which is dominated by mica-rich schist or gneiss derived from shale prololith (Lightfoot et al., 2017; Zwanzig et al., 2007). These ore deposits are the principal mining targets of Thompson mine, as well as the adjacent Birchtree mine which was the location for the recent study of Sherwood Lollar et al. (2021). Thompson mine and Birchtree mines are co-located in the TNB and are only about 5 km away from each other in the same geologic setting.

### 2.2 | Sampling and field measurements

Fracture waters (FW), naturally discharging under artesian conditions from five boreholes at Thompson mine at 1067-m level, were collected in June 2006. A detailed description of these samples is published in a previous study (Telling et al., 2018). For these studies, boreholes were specifically chosen to cover a range of salinities in fracture water measured by in situ conductivity. These boreholes were generally sub-vertical at dip between −63° and −84° from horizontal, with lengths ranging from 227 to 472 m. Drilling water (DW) derived from the surface water sources and circulated down to the mining operation levels was also sampled. The DW sample serves as the contamination endmember to assess the potential contamination in fracture fluid samples as recommended best practice (Sheik et al., 2018 and references therein). The FW samples were collected between 2–10 months after borehole completion.

Water conductivity, pH, and temperature were measured at the point of collection using pre-calibrated portable meters (OAKION, PC450 waterproof handheld meters). Total dissolved oxygen and dissolved hydrogen sulfide content were determined in situ by colorimetric analysis using CHEMet self-filling ampoules (CHEMetrics Inc., USA). The water flow rates were determined by removing 2 L of water from the borehole and recording the time required for the naturally flowing

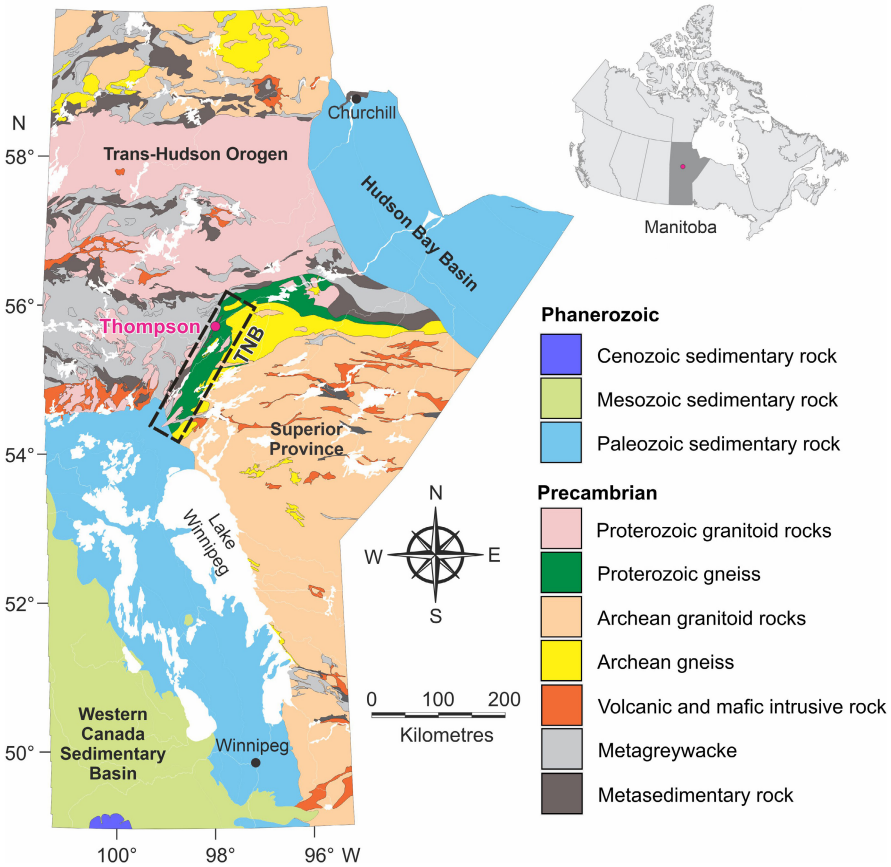


FIGURE 1 Location of Thompson, northern Manitoba, Canada. Geological map modified after Manitoba Geological Survey.

water to refill. Before measuring the gas flow rates, the borehole was sealed using an autoclaved rubber stopper with a tube inserted in it. The gas flow rates were determined by placing the end of the tubing beneath an inverted graduated beaker that was submerged in a bucket filled with water, and recording the time required for the flowing gas to displace a known volume of water in the inverted beaker (Ward et al., 2004). Both measurements were repeated at least three times.

Following gas flow rate measurements, gas samples were collected following the procedures of Ward et al. (2004). Briefly, gases which were collected in the inverted beaker were transferred directly into pre-evacuated 125-mL borosilicate serum vials with butyl blue stoppers through a 22-g syringe needle on a luer attachment at the top of the beaker. The serum vials were acid-washed and pre-fixed with 50-μL saturated $HgCl_2$ solution to prevent any microbial activity post-sampling, after the methods of Ward et al. (2004). All stoppers were pretreated by boiling in 0.1 M NaOH for at least one hour after methods of Oremland and Des Marais (1983). All gas samples were refrigerated until analysis.

Water samples were taken via a sterilized Tygon tube attached to a sterile 60-mL plastic syringe following the methods reported in Telling et al. (2018). Approximately 20 mL of water was filtered through sterilized 0.45 μm cellulose nitrate filters into 30 mL Nalgene bottles and refrigerated until analysis of major cations and anions. 0.1 M of nitric acid (trace metal grade) was added to the cation sample to keep all cations in a dissolved state. Samples for dissolved iron (II) quantification (16 mL) were filtered as above and preserved with 400 μL concentrated HCl (trace metal grade) and refrigerated. Water for ammonia analysis (15–20 mL) was filtered as above and conditioned with 50 μL concentrated $H_2SO_4$ to lower pH to 1.5–2. Water samples for dissolved inorganic carbon (DIC), dissolved organic carbon (DOC), and short-chain organic acid concentrations were filtered through 0.22 μm filters and collected in pre-combusted 20 mL glass vials without headspace and fixed with $HgCl_2$. 50 mL of water sample for MPN analysis was collected from each borehole in 160 mL borosilicate serum vials sealed with butyl rubber stopper, leaving 110 mL of headspace. Before sampling, serum vials were acid-washed and baked overnight at 450°C, and rubber stoppers were pretreated as described above. Vials for aerobic incubations contained ambient air, whereas those for anaerobic incubation were pre-flushed with $N_2$, and pre-conditioned with freshly synthesized FeS to ensure anoxic conditions after the methods of Lollar et al. (2019). 60 mL samples for microbial total cell counts were fixed in the field with 37% formaldehyde (pre-filtered through 0.1 μm filter) into pre-combusted serum vial to give a final formaldehyde concentration of 4%; samples were then refrigerated at ~4°C until enumeration. Lastly, water was sampled for isotopic composition analysis ($\delta^{18}O_{H_2O}$ and $\delta^{2}H_{H_2O}$) in 30 mL Nalgene bottles without headspace and refrigerated until analysis.

## 2.3 | Laboratory analysis

Analysis of major cations, anions and $\delta^{18}O_{H_2O}$, $\delta^{2}H_{H_2O}$ values was performed at the Environmental Isotope Lab of University of Waterloo, Waterloo, Canada, and the results were published in previous studies (Telling et al., 2018; Warr, Giunta, et al., 2021). In brief, major cations were analyzed using Inductively Coupled Plasma Optical Emission Spectrometry (ICP-OES). Major anions were analyzed by Dionex Ion Chromatography (IC). The overall ionic strength of fluids was calculated using PHREEQC. Acetate concentration was determined in separate run by IC after removing $Cl^-$ in the water as described in Telling et al. (2018). Iron (II) concentrations were determined using Ferrozine method following Stookey (1970). The ammonia concentration was determined after Standard Methods Committee of the American Public Health Association American Water Works Association and Water Environment Federation (2018). $\delta^{18}O_{H_2O}$ was analyzed by $CO_2$ equilibration method (Epstein & Mayeda, 1953), and $\delta^{2}H_{H_2O}$ was determined by manganese reduction at 900°C after Coleman et al. (1982). Precisions were ±0.15‰ and ±2‰ for $\delta^{18}O_{H_2O}$ and $\delta^{2}H_{H_2O}$, respectively. Concentrations of DIC and DOC were determined using OI Analytical TOC Analyzer at the Metals, Environmental and Terrestrial Analytical Laboratory (previously known as the Goldwater Environmental Laboratory) at Arizona State University. The DIC content was measured by first acidifying samples with 10% phosphoric acid to release $CO_2$ which was then analyzed by an infrared detector. Sodium persulfate was then added to the solution to oxidize the remaining DOC to $CO_2$ for quantification by infrared detector. $\delta^{13}C$ values of DIC were analyzed at Hatch Lab at University of Ottawa using OI Analytical Aurora Model 1030W TOC Analyser coupled to a Finnigan Mat DeltaPlusXP isotope ratio mass spectrometer. The $2\sigma$ analytical precision was ±0.4‰.

Compositional analysis of gas samples was performed at the Stable Isotope Laboratory at the University of Toronto as described in Sherwood Lollar et al. (2002) and Telling et al. (2018). Concentrations of $CH_4$, $C_2H_6$, $C_3H_8$, $i$-$C_4H_{10}$, and $n$-$C_4H_{10}$ were determined using a Varian 3400 gas chromatography (GC) equipped with a flame ionization detector, and concentrations of $H_2$, He, $O_2$, and $N_2$ were analyzed using a Varian 3800 GC with a micro-thermal conductivity detector. The reproducibility of triplicate analyses for both measurements was ±5%.

## 2.4 | Microbiology

Total planktonic microbial cell numbers were counted using epifluorescence microscopy using a Leica DMRA2 microscope at a magnification of ×1000, using the Acridine Orange Direct Count (AODC) method of Cragg (1994). Briefly, acridine orange-stained aliquots were filtered onto black polycarbonate filters (0.2 μm pore size, 20 mm diameter), and samples were counted in duplicate until 400 cells were counted with a minimum of either 20 fields of view, or 100 fields of view.

Viable cell density responses to different metabolic activity was estimated using the classic culture-dependent MPN technique (Hurley & Roscoe, 1983; Oblinger & Koburger, 1975). MPN is a statistical method based on the random dispersion of microbes per volume in a given sample. It determines the microbial populations in a sample by inoculating an appropriate liquid growth medium,

followed by multiple-replicate serial dilutions to the extent that none of the inocula shows growth response (Blodgett, 2010). The MPNs are estimated statistically according to Equation (1), or by reference to statistical tables (Blodgett, 2010).

$$\sum_{j=1}^{k} \frac{g_j m_j}{1-\exp(-\lambda m_j)} = \sum_{j=1}^{k} t_j m_j \quad (1)$$

Here, $\lambda$ is the cell density; $K$ denotes the number of dilutions; $g_j$ denotes the number of positive tubes in the $j$th dilution; $m_j$ denotes the amount of the original sample in each tube in the $j$th dilution; $t_j$ denotes the number of tubes in the $j$th dilution.

The MPN technique is commonly used in estimating microbial populations in water and food (e.g., Erkmen, 2022). Like any other cultivation techniques, the MPN approach may produce false negatives; for example, laboratory incubation conditions may prevent the growth of certain microorganisms existing in the natural environment. In addition, the MPN technique lacks precision due to limited numbers of replicates for each dilution level, usually three or five replicates; thus, a 95% confidence interval is provided for each estimation (Woodward, 1957). Regardless of these disadvantages, MPN technique is particularly useful with low-biomass samples and samples containing particulate matter that may interfere with other counting techniques (Blodgett, 2010). Previous studies have successfully applied the MPN technique to investigate microbial activity in continental subsurface fracture fluid samples, which are characterized by high particulate content, high salinity, and low biomass that make the extraction of DNA more of a challenge (e.g., Lollar et al., 2019; Pedersen et al., 2014; Sheik et al., 2021; Telling et al., 2018). In the present study, the MPNs are used semi-quantitatively to compare relative responses of in situ microorganisms to different incubation conditions.

Three salt media with different ionic strengths were prepared before fieldwork, representing brackish (0.06 M), saline (0.8 M) and supersaline (2.5 M) conditions based on previous geochemical characterization of the fluids from the site (Table 1; Telling et al., 2018). The composition of the supersaline media was determined based on Precambrian Shield brines analyzed in previous work (Doig et al., 1995; Frape et al., 1984). The pH of media was adjusted to in situ values of 6.5–7 with 0.1 M HCl or NaOH after the addition of all nutrients and substrates as listed in Table 2. This study investigated a total of 13 microbial metabolisms covering both aerobic and anaerobic conditions. These are summarized in Table 2 which outlines the corresponding incubation conditions and the interpretation of positive growth. Each metabolism was performed in all three media to test microbial response to changes in salinity.

This MPN approach was applied to the DW sample as well as all five FW samples as per best practice for environmental controls (Lollar et al., 2019; Sheik et al., 2018). For each sample, per the MPN statistical methodology, MPN dilutions were carried out in triplicate in 5-mL borosilicate serum vials sealed with butyl rubber stoppers. An initial inoculum of 0.5 mL water samples was added into 4-mL media, followed by four levels of 50-fold dilutions. Triplicate 0.2-μm filtered samples were used as controls on reproducibility. The vials were inoculated at room temperature for 6 months, and the vials were monitored for growth as described in Table 2. The detection limit of this method was between 2 and 360,000 viable cells $mL^{-1}$ (Telling et al., 2018). MPNs of $H_2$-utilizing microorganisms, including aerobic $H_2$-oxidizer, autotrophic Fe(III) reducers, autotrophic sulfate reducers and autotrophic methanogens and putative acetogens, were studied in previous work which focused primarily on $H_2$ oxidation (Telling et al., 2018). In this study, additional eight aerobic and anaerobic metabolisms were investigated.

**TABLE 1** Artificial basal salt media with three different ionic strengths.

| | | Brackish (0.06 M) | Saline (0.8 M) | Super saline (2.5 M) |
|---|---|---|---|---|
| NaCl | g/L | 1.3 | 8.2 | 24.7 |
| $CaCl_2{\cdot}6H_2O$ | g/L | 2.9 | 47.1 | 141.1 |
| $MgCl_2{\cdot}6H_2O$ | g/L | 0.05 | 6.8 | 20.5 |
| $NH_4Cl$ | g/L | 0.4 | Not added | Not added |
| KCl | g/L | 0.1 | 0.2 | 0.2 |
| $NaHCO_3$ | g/L | 1.7 | 1.7 | 1.7 |
| pH | | 7.2 | 6.8 | 6.0 |

## 3 | RESULTS

### 3.1 | Aqueous geochemistry characterization

Water isotopes ($\delta^{18}O$ and $\delta^{2}H$) and relative abundance of the major cations and anions can provide an initial indication on the hydrogeological characteristics of groundwater (Figure 2; Figure S1). For example, paleometeoric water recharged from the surface during recent geologic past (<10 s of thousands of years) carries isotope values still reflecting the conditions associated with its recharge from surface, including precipitation, lakes, rivers, oceans and surface groundwaters, and the $\delta^{18}O$ and $\delta^{2}H$ values of meteoric and paleometeoric groundwaters fall along the global or local meteoric waterline (GMWL or LMWL) (Craig, 1961). In contrast, the signature of deep ancient fracture water is frequently characterized by significant $^{18}O$-depletion resulting from long-term water–rock interactions and isotope exchange at low water to rock ratios over geological (Ma) timescales, overprinting the initial signature and placing them to the left and above the GMWL (Frape et al., 2014; Warr, Giunta, et al., 2021).

A strong correlation in $\delta^{18}O_{H_2O}$–$\delta^{2}H_{H_2O}$ and total dissolved solid (TDS) of groundwaters was previously reported at Thompson area (Frape et al., 1984; Warr, Giunta, et al., 2021), which was further extended by more recent data on FW samples from the adjacent Birchtree mine (Warr, Giunta, et al., 2021) (Figure 2a). This correlation was initially suggested to reflect the recharge of local surface water, supported by the intersection of the least saline waters with

**TABLE 2** MPN culture tubes designed to assay for positive growth responses for 13 aerobic and anaerobic metabolisms.

| Metabolisms | Electron donor | Electron acceptor | Additions per 1 L of media | Headspace gas | Assay for growth |
|---|---|---|---|---|---|
| *Aerobic* | | | | | |
| Aerobic general heterotrophs | Glucose, peptone | $O_2$ | Yeast extract, vitamins (1 mL $L^{-1}$), trace elements (10 mL $L^{-1}$) | Air | Visual: media turned from pink to colorless |
| Aerobic $H_2$ oxidizers | $H_2$ | $O_2$ | Vitamins (1 mL $L^{-1}$), trace elements (10 mL $L^{-1}$), resazurin (0.1 mL $L^{-1}$) | Air, overpressurize with $H_2$ to 1.8 atm. | Visual: media turned from pink to colorless. Confirmed by $H_2$ loss by GC-μTCD |
| Aerobic $C_1$–$C_4$ oxidizers | $C_1$–$C_4$ alkanes | $O_2$ | Vitamins (1 mL $L^{-1}$), trace elements (10 mL $L^{-1}$), resazurin (0.1 mL $L^{-1}$) | Air, overpressurize with $C_1$–$C_4$ alkanes mix to 1.8 at. | Visual: media turns from pink to colorless. Confirm by GC |
| *Anaerobic* | | | | | |
| Autotrophic $SO_4^{2-}$ reducers | $H_2$ | $SO_4^{2-}$ | Sodium sulfate (20 mM), FeS (50 μM), iron nail vitamins (1 mL $L^{-1}$), trace elements (10 mL $L^{-1}$), resazurin (0.1 mL $L^{-1}$) | $H_2$, $CO_2$, $N_2$ | Visual: blackening of iron nail, confirmed by $H_2$ loss by GC-μTCD |
| Autotrophic $Fe^{3+}$ reducers | $H_2$ | $Fe^{3+}$ | Ferric citrate (50 mM) vitamins (1 mL $L^{-1}$), trace elements (10 mL $L^{-1}$), resazurin (0.1 mL $L^{-1}$) | $H_2$, $CO_2$, $N_2$ | Visual: positives turned from orange to green to colorless, confirmed by $H_2$ loss by GC-μTCD |
| Autotrophic Methanogens/Autotrophic acetogens | $H_2$ | $CO_2$ | Vitamins (1 mL $L^{-1}$), trace elements (10 mL $L^{-1}$), resazurin (0.1 mL $L^{-1}$) | $H_2$, $CO_2$, $N_2$ | Confirmed by $H_2$ loss by GC-μTCD, and if methane was detected by GC-FID, counted as methanogens; if there was no methane detected, then counted as putative acetogens |
| $C_1$–$C_4$ alkane oxidizing $SO_4^{2-}$ reducers | $C_1$–$C_4$ alkanes | $SO_4^{2-}$ | Sodium sulfate (20 mM), FeS (50 μM) vitamins (1 mL $L^{-1}$), trace elements (10 mL $L^{-1}$), resazurin (0.1 mL $L^{-1}$), iron nail | $CO_2$, $N_2$, $C_{1-4}$ alkanes. Overpressurize with $C_{1-4}$ alkane mix to 1.8 atm. | Visual: blackening of iron nail. Highest dilution positives can be assayed for $SO_4^{2-}$ depletion (IC) and $C_{1-4}$ alkanes (GC) |
| $C_1$–$C_4$ alkane oxidizing $Fe^{3+}$ reducers | $C_1$–$C_4$ alkanes | $Fe^{3+}$ | Ferric citrate (50 mM), vitamins (1 mL $L^{-1}$), trace elements (10 mL $L^{-1}$), resazurin (0.1 mL $L^{-1}$) | $CO_2$, $N_2$, $C_{1-4}$ alkanes. Overpressurize with $C_{1-4}$ alkane mix to 1.5 atm. | Visual: positives turn from orange to green to colorless. Highest dilution positives can be assayed for $C_{1-4}$ alkanes by GC |
| General fermenters | Glucose, peptone | Glucose, peptone | 10 g glucose, 5 g peptone, 0.1 g yeast extract, vitamins (1 mL $L^{-1}$), trace elements (10 mL $L^{-1}$), 2 drops bromocresol purple | $CO_2$, $N_2$ | Visual: acidification —media turns yellow. Also, gas production by floating of Durham tubes |

TABLE 2 (Continued)

| Metabolisms | Electron donor | Electron acceptor | Additions per 1 L of media | Headspace gas | Assay for growth |
|---|---|---|---|---|---|
| Heterotrophic $SO_4^{2-}$ reducers | Acetate, lactate, pyruvate | $SO_4^{2-}$ | Sodium sulfate (20 mM), Sodium acetate (10 mM), sodium lactate (10 mM), sodium pyruvate (10 mM), FeS (50 μM), iron nail vitamins (1 mL $L^{-1}$), trace elements (10 mL $L^{-1}$), resazurin (0.1 mL $L^{-1}$) | $CO_2$, $N_2$ | Visual: blackening of iron nail |
| Heterotrophic $Fe^{3+}$ reducers | Acetate, lactate, pyruvate | $Fe^{3+}$ | Ferric citrate (50 mM), sodium acetate (10 mM), sodium lactate (10 mM), sodium pyruvate (10 mM) vitamins (1 mL $L^{-1}$), trace elements (10 mL $L^{-1}$), resazurin (0.1 mL $L^{-1}$) | $CO_2$, $N_2$ | Visual: positives turn from orange to green to colorless |
| Heterotrophic methanogens | Acetate, methanol | Acetate, methanol | Sodium formate (40 mM), Sodium acetate (10 mM), methanol (10 mM), FeS (50 μM) | $CO_2$, $N_2$ | Methane detection by GC-FID |

the LMWL (Frape et al., 1984). While the water isotopes of the DW, which is typically recirculated surface water, were not reported in the earlier study, the present study shows that the $\delta^{18}O_{H_2O}$ and $\delta^{2}H_{H_2O}$ signatures of DW at both Thompson and Birchtree mines are consistent with sources from local surface water, for example, similar isotopic composition as the local Burntwood River (Gibson et al., 2021) (Figure 2a). These new data suggest that some of the current study's samples are mixing with surface water or DW (Figure 2a). Since the larger trend of mixing (blue dashed line) indicates a more negative intersection with the LWML than can be accounted for by modern surface water, and given the absence of detectable $^{3}H$ in some of those samples (Frape et al., 1984), the least saline waters may in fact be due to mixing with paleometeoric water recharged in the geologic past, a pattern that has been identified at other subsurface groundwater sites around the world (Borgonie et al., 2019; Heard et al., 2018; Kietäväinen et al., 2013; Onstott et al., 2006; Ward et al., 2004; Warr, Giunta, et al., 2021).

The five fracture water samples investigated in this study had a wide range of TDS content ranging from 28 to 205 g/L, corresponding to ionic strengths of 0.6 M to 6.4 M (Table 3, Telling et al., 2018). As expected, the DW had a considerably lower TDS of 0.04 g/L and relative ionic strength of 0.002 M (Table 3). Results show that water isotopes of the three more saline FWs, that is, FW 1163930, FW 1065760, and FW 1065750 (or alternatively termed as FW#3, #4, and #5 henceforth), fall approximately along the broader correlation trend line as shown by the blue dashed line in Figure 2. In contrast, the two less saline FWs, that is, FW 1065800 and FW 1163630 (or alternative termed as FW#1 and #2 henceforth) trend towards mixing with the DW endmember (grey arrow). Relative proportions of the major cations $Ca^{2+}$ and $Na^{+}$, and the bicarbonate anion (DIC) also showed that FW#2 and particularly FW #1 trend away from the other three more saline water samples and toward the DW (Figure 2b). Clearly these two less saline water samples FW#1 and #2 were likely contaminated by the DW, whereas the three more saline samples FW#3, #4, and #5 were more broadly reflective of the natural mixing between subsurface brine and (paleo)meteoric water.

The DOC contents were between 0.6 and 1.6 mM in FW#3, #4, and #5, but were significantly higher (10.9–38.6 mM) in samples FW #1 and #2 (Table 3). Similarly high DOC was recently observed in deep brines of Moab Khotsong gold mine (2.9–3.1 km below land surface) (Nisson, Kieft, et al., 2023). Acetate concentrations in all FW samples were between 53 μM and 496 μM, in a similar range as those detected at the adjacent Birchtree mine in the Thompson area (Sherwood Lollar et al., 2021), with the highest concentration observed in FW#1. Formate was detected in all FW samples (<2–41 μM), while propionate and butyrate concentrations were generally below 1 μM (Table 3). The highest concentration of sulfate was detected in FW#2, followed by the most saline sample FW#5. In addition, the total dissolved nitrogen was comprised of generally low concentrations of $NH_4^{+}$, $NO_3^{-}$, and $NO_2^{-}$ (Table 3). Although FW#1 and #2 were likely contaminated by DW based on their $\delta^{18}O_{H_2O}$ and $\delta^{2}H_{H_2O}$ values, the generally much lower concentrations of DOC and acetate in the DW suggest the latter is not a major source of these DOC species in any FW samples (Table 3).

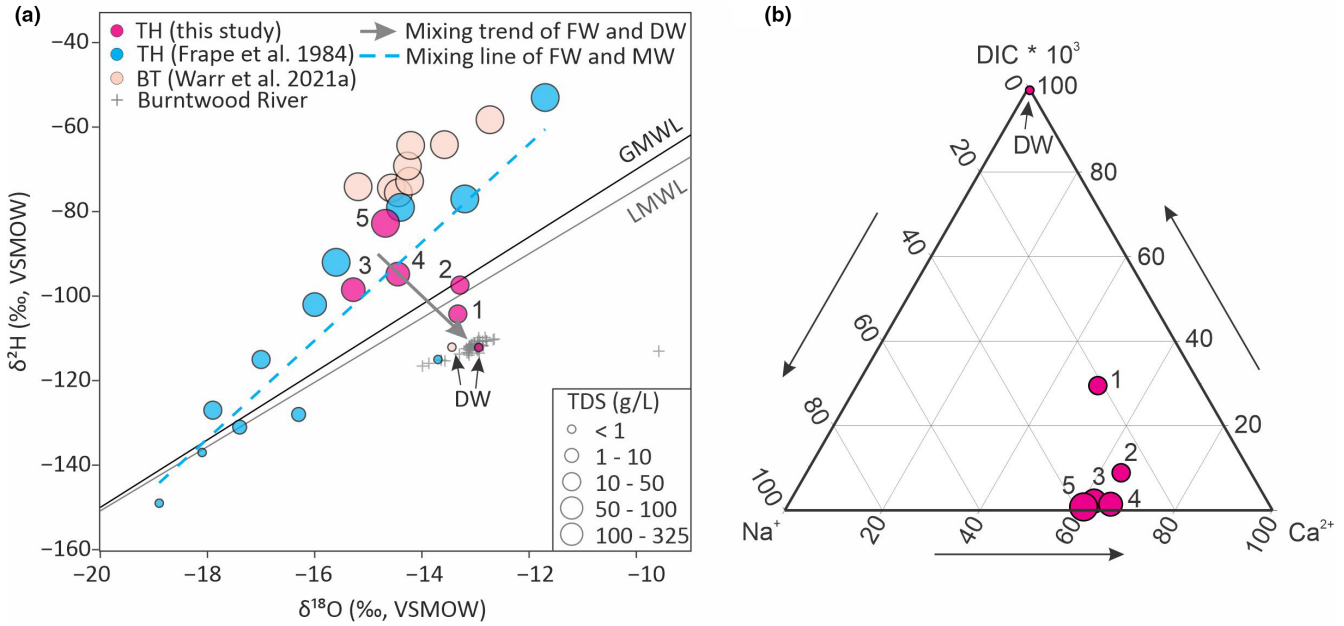


FIGURE 2 Isotopic values and aqueous geochemical results of fracture water samples and drilling water from Thompson area, Manitoba, Canada. (a). Isotopic values of water samples. The symbol size corresponds to the content of total dissolved solids (TDS) in each sample per the inset. The numbers besides data indicate fracture water (FW) samples in this study from Thompson mine (TH) (dark pink circles) with increasing salinities from FW#1 to FW#5 (number 1 to 5 on the plot). This plot also shows previous samples at Thompson mine from Frape et al. (1984) (blue circles) at various depths ranging from 50 m to 1.5 km below surface, and samples from the nearby Birchtree mine (BT) (light pink circles) located at 1.2 km depth level (Warr, Giunta, et al., 2021). Monthly water isotopes of the nearby Burntwood River were analyzed from 2014–2018 (mean value of $\delta^2H$ is −112.2‰ and of $\delta^{18}O$ is −12.99‰) reflecting modern local meteoric water (Gibson et al., 2021). The global meteoric water line (GMWL: $\delta^2H = 8\ \delta^{18}O + 10$, Craig, 1961), and local meteoric water line (LMWL: $\delta^2H = 7.61\ \delta^{18}O + 1.29$, $R^2 = .99$), are plotted for context. The LMWL was calculated from monthly precipitation water isotopes at Manitoba monitored from 1975 to 1993 (IAEA WISER database). Blue dashed trend line shows an approximate mixing between brines and paleometeoric water. Grey arrow shows that based on $\delta^{18}O$ and $\delta^2H$ values, at least FW#1 and FW#2 from this study were influenced by mixing with drilling water (DW) derived from local surface waters. This is consistent with their lower ionic strength and detectable dissolved oxygen, compared to the three other FW samples (Table 3). (b) Ternary plot of $Ca^{2+}$, $Na^+$, and dissolved inorganic carbon (DIC) of water samples. See also Table 3. Milliequivalents per liter of DIC (calculated as $HCO_3^-$) in FW samples are orders of magnitude lower than their corresponding $Ca^{2+}$ and $Na^+$, therefore are multiplied by 1000 to better show the different trends between samples. The symbol size corresponds to TDS of each sample as per panel a.

The total DIC concentrations of the least saline samples, FW#1, and #2 (125 and 164 μM) were at least three-fold higher than those of the more saline samples, while DIC content of the DW also fell within this range (151 μM) (Table 3). The three more saline FW samples (FW#3, #4, and #5) had DIC concentrations an order of magnitude lower between 28–39 μM. Overall, the DIC content of FWs in the present study was in a similar range as that of saline waters from Birchtree (31–250 μM; Sherwood Lollar et al., 2021), but unlike Birchtree saline water, DIC in most of the fracture samples of this study was more $^{13}C$-depleted, with $\delta^{13}C$ values in the range of −30 to −20‰, except for FW#3 (−9.4‰) (Table 3).

## 3.2 | Gas compositions

The highest $H_2$ concentration was found in the most saline sample FW#5 (2.7%), coinciding with previous work where elevated $H_2$ concentrations were typically found in the deeper and highly saline fracture waters (Onstott et al., 2006; Sherwood Lollar et al., 2007). The He content was in the range of 2.4%–3.3%, $N_2$ in the range of 49%–62%, while $C_1$–$C_4$ alkanes accounted for 36%–48% of total detected gas and were dominated by methane (>92%) and ethane (>4.0%). $O_2$ was detected in all samples, with the highest content detected in FW#5 (6.5%) (Table 3). This may partly be due to air introduction during sampling, given that dissolved $O_2$ in the more saline FW#3, #4, and #5 were below detection limit. Only FW#1 and FW#2 as well as DW had dissolved oxygen levels above detection limit (Table 3). Due to uncertainties in relative contribution of air-borne oxygen to the samples, no air-correction calculation was applied for the gas compositions listed in Table 3.

## 3.3 | Planktonic microbial cell densities

Total planktonic cell numbers in FW samples ranged by four orders of magnitude (Figure 3d and Table S1). The most saline FW#5 had the lowest cell density of $10^3$ cells $mL^{-1}$, which is in a similar range as other

low-biomass deep subsurface communities identified globally (e.g., Lollar et al., 2019; Magnabosco et al., 2018; Nyyssönen et al., 2014). Higher cell densities of $10^5$–$10^6$ cells $mL^{-1}$ were found in samples FW#4 and #3. These two samples had lower ionic strengths and more negative $\delta^2H$ values than FW#5, and may reflect a larger component of the paleometeoric water component identified by Frape et al. (1984) than found in the most saline sample FW#5 (Figure 2). By comparison, the samples with the lowest ionic strengths, FW#2 and #1, that may be most influenced by mixing with DW, had the highest cell density of $10^6$–$10^7$ cells $mL^{-1}$ among the fracture fluids, approximately 10-fold higher than the cell density of $10^5$–$10^6$ cells $mL^{-1}$ in the DW (Figure 3d).

## 3.4 | MPN results

All MPN results with 95% confidence intervals are presented in Table S1, and the mean values are displayed graphically in Figure 3. In this study, the FW and DW samples were inoculated in pre-prepared brackish, saline, and supersaline media with respective solution ionic strengths of 0.06 M, 0.8 M, and 2.5 M. These experiments were designed to test the response of various microbial metabolisms in each fluid type and to investigate the effect of different salinity levels on microbial activity. Accordingly, the supersaline medium represents the salinity condition that is most close to the in situ salinity of FW#2, #3, #4, and #5, which have respective in situ ionic strengths of 1.9 M, 2.5 M, 2.7 M, and 6.4 M. Whereas for the least saline FW#1 (ionic strength of 0.6 M) and the drilling water (ionic strength of 0.002 M), the respective saline and brackish medium is closest to their in situ conditions.

### 3.4.1 | Aerobic metabolisms

For the three MPN metabolisms investigated under aerobic conditions, that is, aerobic $H_2$ oxidation, $C_1$–$C_4$ oxidation, and heterotrophy, the aerobic heterotrophs dominated all water samples in all three types of cultivation media (Table S1). While aerobic $C_1$–$C_4$ oxidation was not detected in any samples, aerobic $H_2$ oxidation was only detected in FW#1, #2, and DW in brackish media. Although FW#1 under brackish condition had the highest MPNs associated with aerobic $H_2$ oxidation among all samples, these MPNs were still at least 100-fold lower than those of the aerobic heterotrophs in the same sample under same salinity conditions (Table S1). Notably, the DW and the least saline samples (to the left of vertical dashed lines in Figure 3a–d) were substantially different from samples that were largely uncontaminated by DW (to the right of the vertical dashed lines) based on the discussion in Section 3.1. DW, FW#1, and #2 showed strong response from aerobic heterotrophs in the MPNs. Specifically, for the least saline FW#1, cell densities of aerobic heterotrophs remained above the upper detection limit in both saline and brackish media but dropped significantly in supersaline medium (Figure 3a). For FW#2, aerobic heterotrophs were above the upper detection limit in all three media, and changes in media salinity did not seem to notably affect their growth (Figure 3a). In contrast, samples FW#3, #4, and #5 showed lower microbial responses in most of the media. Significantly, FW#3, #4, and #5 showed the lowest MPN responses in the brackish media, and for the most saline FW#5, dilution of media solution led to progressive decrease in the already low abundance of the aerobic heterotrophs (Figure 3a). This suggests, for the uncontaminated, more saline fracture waters (FW#3, #4, and #5), their indigenous microbial populations do not respond well to lower salinity culture conditions. DW notably showed the opposite pattern whereby aerobic heterotrophic response was highest in the lowest ionic strength condition, and response dropped dramatically in the saline, and particularly supersaline media conditions, suggesting the DW microflora could not grow well under high salinity conditions (Figure 3a).

### 3.4.2 | Anaerobic metabolisms

For the 10 MPN experiments under anaerobic cultivation conditions, it is notable that neither the DW, nor the least saline FW sample FW#1, showed any MPN response when grown under the supersaline media conditions (2.5 M) (Figure 3b). Furthermore, the metabolic diversity of the MPN responses for these two samples under brackish conditions are relatively similar (Figure 3c), suggesting the DW contamination of FW#1 includes likely an impact on the microflora in this sample. Overall, these are the most diverse MPN responses seen in this study (Figure 3b,c). On the other hand, in more saline media that were most close to their in situ ionic strength, 0.8 M and 2.5 M, respectively, both FW#1 and #2 tended towards high relative abundance and dominance of heterotrophic sulfate reducers (Figure 3c). The total anaerobic MPNs of heterotrophic sulfate reducers in these samples were up to four orders of magnitude higher than those in the DW in both brackish and saline media (Figure 3b). In addition, general fermentative microorganisms and heterotrophic iron reducers observed in the FW#1 cultivated in saline media (0.8 M) were two orders of magnitude higher than those detected in the DW (Figure 3b,c; Table S1). These results suggest that while impacted by mixing with DW, likely some of the MPN responses for FW#1 and #2 nonetheless reflect native microflora.

As noted in Section 3.4.1, the strongest evidence of likely native microflora response is found in more saline samples FW #3, #4, and #5. Lower microbial metabolic diversity and lower biomass was detected in samples FW#3, #4, and #5 (Figure 3c,d), and responses were dominated by general fermenters and to a lesser degree, heterotrophic sulfate reducers (Figure 3c). In supersaline media that were most close to their in situ salinity conditions, no MPN responses were detected in FW#4 and #5, while only low abundances of heterotrophic sulfate reducers were detected in FW#3 (Figure 3b,c). In saline and brackish media, increasing MPN response from general fermenters were detected in FW#4 and #3, which was three orders of magnitude higher than those detected in the DW (Figure 3b,c; Table S1). For the most saline FW#5, only minor amounts of fermentative microorganisms were detected in brackish medium, lower than those detected in the DW (Figure 3b,c; Table S1).

Finally, MPNs for $H_2$-utilizing sulfate reducers and putative acetogens had strong response only in brackish cultivation media in

TABLE 3 Aqueous and gas geochemistry of Thompson fracture fluids and drilling water.

| Samples | | FW 1065800 | FW 1163630 | FW 1163930 | FW 1065760 | FW 1065750 | Drilling water |
|---|---|---|---|---|---|---|---|
| **Alternative ID** | | **FW#1** | **FW#2** | **FW#3** | **FW#4** | **FW#5** | **DW** |
| BH completion date | | 29-Apr-06 | 16-Mar-06 | 26-Aug-05 | 7-Apr-06 | 27-Mar-06 | – |
| Sampling date | | 13-Jun-06 | 13-Jun-06 | 14-Jun-06 | 14-Jun-06 | 13-Jun-06 | 14-Jun-06 |
| Borehole length | m | 227 | 274 | 472 | 267 | 265 | – |
| Borehole dip | ° | −84 | −65.4 | −63 | −76.2 | −80 | – |
| *Aqueous geochemistry* | | | | | | | |
| Water flow rate | mL/min | 20–40 | 20–40 | 20–40 | 20–40 | 20–40 | - |
| Temperature | °C | 22 | 22 | 22 | 22 | 22 | 25 |
| pH | | 6.8 | 6.8 | 6.4 | 7.2 | 6.3 | 7.1 |
| Conductivity | mS/cm | 38 | 80.4 | 89.4 | 93.5 | 120 | 0.5 |
| TDS | g/L | 28 | 40 | 84 | 90 | 205 | 0.04 |
| Ionic strength | M | 0.6 | 1.9 | 2.5 | 2.7 | 6.4 | 0.002 |
| $Li^+$ | mM | <0.4 | <0.4 | <0.4 | <0.4 | <0.4 | <0.001 |
| $Na^+$ | mM | 117 | 376 | 620 | 605 | 1368 | 0.18 |
| $K^+$ | mM | <0.3 | 1.9 | 2.2 | 1.6 | 10 | 0.03 |
| $NH_4^+$ | mM | <0.8 | <0.8 | <0.8 | <0.8 | <0.8 | <0.003 |
| $Mg^{2+}$ | mM | 8.6 | 22 | 37 | 35 | 162 | 0.18 |
| $Ca^{2+}$ | mM | 138 | 456 | 544 | 616 | 1086 | 0.43 |
| $Fe^{2+}$ | mM | 0.01 | 0.02 | 0.2 | 0.03 | 0.17 | 0.004 |
| $Cl^-$ | mM | 539 | 336 | 1296 | 1403 | 3513 | 0.21 |
| $Br^-$ | mM | 1.1 | 3.6 | 6.0 | 5.7 | 11 | <0.003 |
| $NO_3^-$ | mM | <0.09 | 0.5 | <0.09 | <0.09 | <0.09 | <0.004 |
| $NO_2^-$ | mM | <0.13 | <0.13 | <0.13 | <0.13 | <0.13 | <0.004 |
| $HPO_4^{2-}$ | mM | <0.17 | <0.17 | <0.17 | <0.17 | <0.17 | <0.007 |
| $SO_4^{2-}$ | mM | <0.08 | 0.41 | <0.08 | <0.08 | 0.11 | 0.09 |
| Formate | μM | <2 | 11 | <2 | 41 | 19 | 7 |
| Acetate | μM | 496 | 67 | 82 | 57 | 53 | 5.0 |
| Propionate | μM | <1 | <1 | <1 | <1 | <1 | <1 |
| Butyrate | μM | <1 | <1 | <1 | <1 | <1 | <1 |
| DOC | μM | 10,863 | 38,578 | 601 | 641 | 1615 | 522 |
| DIC[a] | μM | 164 | 125 | 39 | 28 | 30 | 151 |
| Dissolved $O_2$ | μM | 30[b] | 30[b] | <30 | <30 | <30 | 200[b] |

TABLE 3 (Continued)

| Samples | | FW 1065800 | FW 1163630 | FW 1163930 | FW 1065760 | FW 1065750 | Drilling water |
|---|---|---|---|---|---|---|---|
| **Alternative ID** | | **FW#1** | **FW#2** | **FW#3** | **FW#4** | **FW#5** | **DW** |
| Dissolved sulfide[c] | μM | <3 | 88–147 | <3 | <3 | <3 | <3 |
| $\delta^{13}C_{DIC}$ | ‰ | −20.6 | −30.3 | −9.4 | −19.9 | −33.7 | −7.7 |
| $\delta^{18}O_{H_2O}$ | ‰ | −13.3 | −13.3 | −15.3 | −14.5 | −14.7 | −12.9 |
| $\delta^{2}H_{H_2O}$ | ‰ | −104.2 | −97.4 | −98.5 | −94.8 | −82.8 | −112.2 |
| *Gas compositions* | | | | | | | |
| Gas flow rate | mL/min | ~0.3 | 44–46 | ~7 | ~0.1–0.3 | ~0.3 | NA |
| $H_2$ | vol% | 0.03 | 0.3 | 0.9 | 0.8 | 2.7 | NA |
| He | vol% | 2.8 | 3.0 | 3.3 | 2.7 | 2.4 | NA |
| $O_2$ | vol% | 2.3 | 0.9 | 0.7 | 0.9 | 6.5 | NA |
| $N_2$ | vol% | 49.0 | 59.2 | 52.9 | 62.2 | 52.5 | NA |
| $CH_4$ | vol% | 45.5 | 36.6 | 43.8 | 36.5 | 34.7 | NA |
| $C_2H_6$ | vol% | 1.9 | 2.9 | 2.7 | 2.8 | 1.7 | NA |
| $C_3H_8$ | vol% | 0.15 | 0.29 | 0.23 | 0.23 | 0.1 | NA |
| *i*-$C_4H_{10}$ | vol% | 0.009 | 0.022 | 0.016 | 0.021 | 0.004 | NA |
| *n*-$C_4H_{10}$ | vol% | 0.015 | 0.042 | 0.022 | 0.036 | 0.008 | NA |

Abbreviation: NA, not analyzed.

[a]Calculated as $HCO_3^-$.

[b]Corresponding to 12%, 13%, and 55% $O_2$ saturation for FW#1, #2, and DW.

[c]Calculated as $H_2S$.

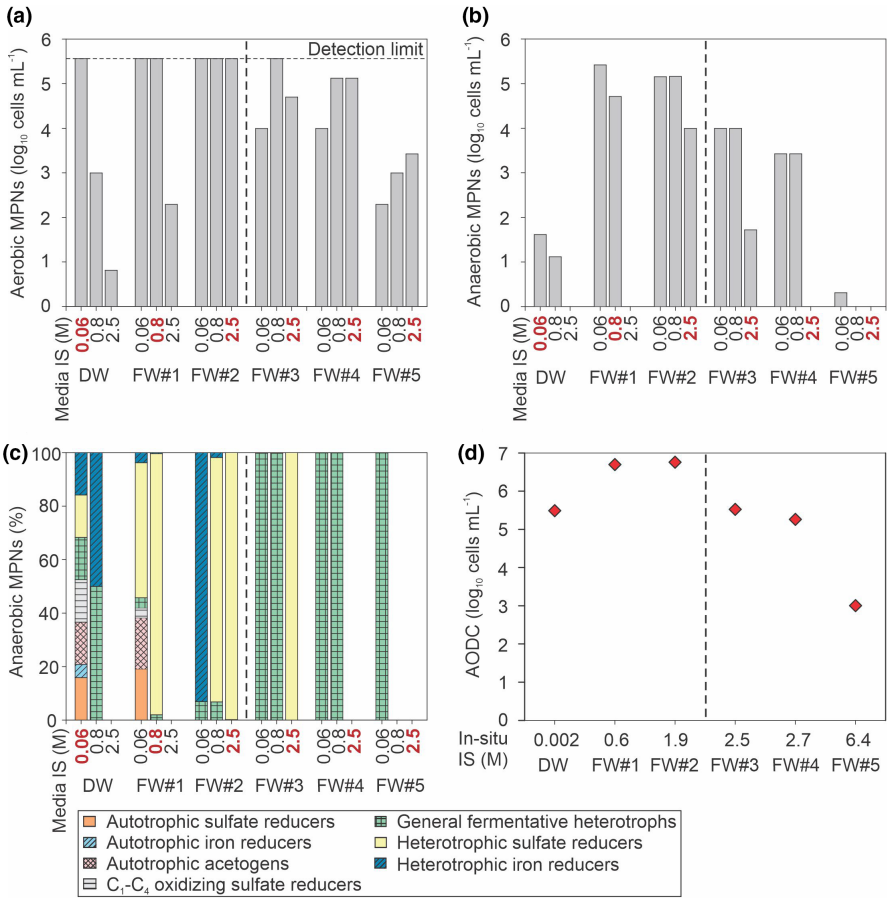


**FIGURE 3** The total and relative viable cell densities based on MPN, and total cell counts using AODC in water samples from Thompson. For MPN experiments, all samples were inoculated in brackish, saline and supersaline media with respective ionic strengths (IS) of 0.06 M, 0.8 M and 2.5 M. The media with IS most close to in situ conditions of corresponding samples are highlighted in red and bold on *x*-axis. (a) Total aerobic MPNs. More than 97% of detected aerobic MPNs were aerobic heterotrophs with minor amounts of aerobic $H_2$ oxidizer in FW#1, #2 and DW, under 0.06 M condition (see Table S1). (b) Total anaerobic MPNs. (c) Relative abundance of anaerobic MPNs. (d) Total cell counts. The detection limit of MPNs is between 2 and 360,000 viable cells $mL^{-1}$, and reported data are based on mean values, the corresponding 95% confidence interval for each estimate is reported in Table S1. DW and DW-impacted samples are on the left-hand side of the vertical dashed line (see text for discussion).

FW#1, which were approximately four orders of magnitude higher than those in the DW. These $H_2$ utilizing metabolic responses did not actively occur at detectable levels (≤20 cells $mL^{-1}$) in more saline FWs or cultivation media within experimental timeframes (Figure 3b,c; Table S1). In addition, MPNs of hydrogenotrophic (autotrophic) methanogens were found only once in this study, and only just above the lower detection limit (for FW#2) in supersaline medium (2 cells $mL^{-1}$; Table S1). The $H_2$-utilizing iron reducers were detected in DW, FW#1, and #2 with low level of MPNs (< 10 cells $mL^{-1}$). These observations are broadly consistent with a previous MPN and microcosm study by Telling et al. (2018) which showed undetectable $H_2$ utilization in samples with ionic strengths >1.9 M under both aerobic and anaerobic conditions. The MPNs of heterotrophic methanogens (using acetate and/or methanol) were only detected at low values in diluted media of FW#2 and #3 (< 10 cells $mL^{-1}$; Table S1). Lastly, while $C_1$–$C_4$ oxidation coupled to sulfate reduction had strong response in brackish medium for FW#1, only low levels of MPNs were detected in saline medium for FW#1, as well as brackish media for both DW and FW#2 (≤20 cells $mL^{-1}$). MPNs of $C_1$–$C_4$ oxidizing iron reducers were below detection limit (Figure 3b,c; Table S1) in all samples except FW#1 in brackish medium. A full list of the MPNs for each metabolism is provided in Table S1.

## 4 | DISCUSSION

### 4.1 | Native microbial flora in fracture waters at Thompson

#### 4.1.1 | Aerobic and facultative anaerobic heterotrophs

As noted in Section 3.1, the geochemical evidence on potential impact of drilling water on the natural fracture waters sets the stage for the discussion of microbiology results. By comparing results from both the DW-impacted (FW#1 and #2) and unimpacted fracture

waters (FW#3, #4, and #5), it is possible to decipher the potential effects of mining activity on subsurface biosphere, also to provide indicator of contamination for future study. The strong responses from aerobic heterotrophs in DW and DW-impacted FW#1 and #2 are consistent with the aerobic to microaerobic nature of the fluids, as shown by the detectable dissolved oxygen in the fluids (Table 3), possibly related to the introduction of DW. It is notable that MPN responses for the DW were only strong when cultured in brackish medium and dropped off significantly under ionic strength ranges of 0.8–2.5 M reflective of the fracture fluids. In contrast, in saline and supersaline media, both FW#1 and especially FW#2 had significant MPN responses for aerobic heterotrophs (Figure 3a), suggesting that some of the aerobic heterotrophs in samples FW#1 and FW#2 may represent native communities that are more saline tolerant than those present in the low ionic strength DW. It is likely however that these samples are heavily impacted by the mixing with DW (and associated microbial communities in the DW), and hence, the focus of the microbial interpretation for this study will be on the three samples that fall along the Frape et al. (1984) mixing line between saline brines and paleometoeric waters (blue hatched line in Figure 2). Some impact of DW mixing in samples FW#3, #4, and #5 cannot be ruled out, but as discussed in Section 3.1, there is no evidence for such contamination based on the isotopic and geochemical data.

In contrast to FW#1 and #2, the MPN responses for aerobic heterotrophs in FW#3, #4, and #5 had the lowest responses in the brackish media and, for the most saline FW#5, increasing dilution of ionic strength appeared to inhibit microbial response (Figure 3a). These results suggest the presence of indigenous halophiles in these more saline FWs which are poorly adapted to grow in less saline conditions. Given that concentrations of dissolved oxygen were below detection limit in all three of these samples (Table 3), the apparent detection of aerobic heterotrophs in these samples may also hint at the presence of facultative anaerobic heterotrophs. Several of the early studies of microbiomes in the deep continental subsurface emphasized both the reduced and oligotrophic nature of the fracture fluids and a general dominance of $H_2$-utilizing sulfate reducing bacteria and/or methanogens in deep and hydrogeologically isolated subsurface waters (Chivian et al., 2008; Lin et al., 2006; Magnabosco et al., 2016). More recently, in less hydrogeologically isolated settings, more complex and diverse microbial ecosystems have been unveiled. Lau et al. (2016) reported a highly diverse microbial communities in a subsurface site of South Africa, consisting of sulfate reducers, methanogens, methanotrophs, and most importantly, the dominance of sulfur oxidizing bacteria coupled with denitrification. This revealed a redox potential much higher on the redox (Eh) ladder than previously expected in a subsurface setting. Ruff et al. (2023) furthered supported this interpretation by reporting that even in old and supposedly anoxic groundwaters, oxygen can be produced in situ through microbial dismutation of chlorite and nitric oxide, thus supporting a series of hitherto underappreciated aerobic microbial activities via what they called "dark oxygen". Other studies have also reported aerobic metabolic potential in deep terrestrial subsurface settings, including several deep aquifers in the Fennoscandian Shield where viable methanotrophic bacteria were detected (Chi Fru, 2008), and artesian water samples from a 2.8-km-deep borehole in Western Siberia, Russia, where substantial amounts of heterotrophic bacteria capable of aerobic respiration were reported (Kadnikov et al., 2020). While oxygen and aerobic organisms could be delivered to the subsurface by penetration of (paleo)meteoric waters (Borgonie et al., 2011, 2015) and likely are in some cases, the recent work also suggests for other hitherto underappreciated oxidant sources. In addition to in situ microbial production of oxygen (Kraft et al., 2022; Ruff et al., 2023), the presence of oxygen and other subsurface oxidants can also be attributed to geochemical and geologic processes such as water radiolysis (Li et al., 2016; Lin, Hall, et al., 2005; Lin, Slater, et al., 2005; Sauvage et al., 2021), and stress-induced generation via silicate mineral - water interactions (e.g., He et al., 2021, 2023; Stone et al., 2022). The aerobic heterotrophs detected in the MPN results of this study suggest that external sources, for example, from (paleo)meteoric water, and potentially in situ production subsurface oxidants for instance through radiolysis (Li et al., 2016) may support a more significant role for aerobic metabolisms than have been previously appreciated in the deep subsurface biosphere.

### 4.1.2 | Strong responses from heterotrophic sulfate reducers and general fermenters under anaerobic conditions

Under anaerobic conditions, the heterotrophic sulfate reducers dominated in FW#1 and #2 under those ionic strengths closest to their respective in situ ionic strength (Figure 3c,d). When cultured under the lowest ionic strength (0.06 M), the MPN responses were lower for heterotrophic sulfate reducers, and a wider range of metabolic responses were seen – and in particular, for FW#2, an increase in heterotrophic iron reduction. Taken together, these results suggest heterotrophic sulfate reducers form an important, though not exclusively dominant component of the native microbial flora in these two samples. FW#1 shows additional metabolisms including autotrophic $H_2$-utilizing sulfate reducers and autotrophic putative acetogens (Figure 3b,c), but with responses up to four to five orders of magnitude higher than those detected in DW, suggesting these microorganisms may represent components of the native microbial flora. In contrast, not only were anaerobic MPN responses much lower in all DW cultures (Figure 3b), but responses reflected a much larger range of metabolisms in DW (Figure 3c). As noted in the discussion of aerobic metabolisms, there is likely a significant impact of mixing with DW in FW#1 and #2 and the microbial MPN responses may reflect that intermediate (mixed) condition of these samples.

The DW-unimpacted FWs (#3, #4, and #5; to the right of the vertical hatched line) showed generally lower MPN responses under anaerobic conditions compared to aerobic conditions (Figure 3a,b) and lower direct cell counts (Figure 3d). In supersaline media that are most close to in situ salinity conditions, the heterotrophic sulfate reducers exclusively dominated FW#3, although their MPNs were

approximately two orders of magnitude lower compared to FW#1 and #2 (Figure 3b,c). Otherwise, FW#3 as well as FW#4 and #5 were dominated by general fermenters in diluted media. The relatively low MPN response of fermentative heterotrophs in the supersaline media of FW#3 and #4, and in the brine FW#5 (Figure 3) may due to the high bioenergetic cost on osmolyte synthesis, which is essential for subsurface fermentation (Borton et al., 2018; Daly et al., 2016). It is important to note that MPN results are always affected by the possibility of false negatives. Given in particular the known slow rate of metabolism in deep subsurface communities (Lin et al., 2006; Trembath-Reichert et al., 2021), the possibility that the culturing technique failed to capture slowly metabolizing microbial community members during the short experimental timeframe must always be considered. Collectively, the dominance of heterotrophic sulfate reducers and general fermenters likely reflects an indigenous community in FW#3, #4, and #5 that are largely unimpacted by DW. While this study suggests that the heterotrophic sulfate reducers present in these fracture fluids may be more saline tolerant than general fermenters, the general fermenters showed potential greater adaptability to lower ionic strength conditions within the experimental timeframe.

The generally low MPN response observed for $H_2$-driven metabolic processes under the more saline conditions tested here may be related to the higher potential bioenergetic cost of organic osmolyte synthesis at increasing ionic strengths (Telling et al., 2018). $H_2$-utilizing sulfate reducers might be hindered by sulfate limitation, as the presence of high dissolved organic carbon levels may preferentially support the observed more active heterotrophic sulfate-reducing microorganisms which compete for available sulfate. Other $H_2$-utilizing metabolisms such as hydrogenotrophic methanogens or acetogens would require DIC as the electron acceptor. While they cannot be entirely ruled out, if abundant, their activity should typically lead to more enriched $\delta^{13}C_{DIC}$ values than those observed in these fluids (Table 3). It should be noted that the presence of acetoclastic methanogenesis in these fluids was previously suggested based on positive relationships between $\delta^{13}$C-DIC and $\delta^{13}$C-acetate in samples from the adjacent Birchtree mine (Sherwood Lollar et al., 2021). The detection of only very low corresponding MPNs of these groups in this study, that is, heterotrophic methanogens using acetate and/or methanol, may be due to a false negative result from the cultivation method that does not optimize for syntrophic partnerships between metabolically different microbial groups. Alternatively, it is also possible that methanogens were outcompeted by other heterotrophic microorganisms. It is notable however that acetoclastic methanogens were found only in the fracture waters and not the DW (Table S1), once again suggesting the presence of a native microflora.

### 4.1.3 | Dominance of heterotrophy over chemoautotrophy

In addition to the large response from aerobic metabolism, a feature of the detected anaerobic microbial metabolisms in FW samples at Thompson is the observed overall greater role of heterotrophy at this site than has been typically described for other deep subsurface biosphere sites investigated to date (e.g., Chivian et al., 2008; Lin et al., 2006; Lollar et al., 2019). In subsurface settings that are largely isolated from surface hydrologic cycles over long geologic time scales at tens of millions to billions of years, the ecosystems have often been considered to be principally chemosynthetic in nature, driven by long-term geological water-rock reactions (Li et al., 2016; Lin, Hall, et al., 2005; Sherwood Lollar et al., 2014). Here at Thompson, the more hydrogeologically open nature of the system, with the substantial mixing between deep saline fluids and paleometeoric waters shown in Figure 2 may play a role in the different characteristics of this subsurface biome.

One of the features in geochemistry of Thompson fracture fluids that supports dominance of heterotrophy, in particular sulfate reduction and fermentation, is the high concentrations of DOC in the fracture fluids. Some portion of this DOC pool could supply carbon and energy sources for microbial fermentation (Bomberg et al., 2021). Fermentation is identified as a major metabolic activity in heterotrophic dominating subsurface environments, which metabolize the significant complex organic matter in the DOC pool into small organic compounds that can then be utilized by different types of microorganisms including sulfate reducers (Bomberg et al., 2021; Lovley & Chapelle, 1995). In the meantime, heterotrophic sulfate reducing microorganisms could couple sulfate reduction to the oxidation of a range of organic compounds including acetate and potentially, those delivered by fermentation, consistent with the dominance of both fermentation and heterotrophic sulfate reduction in Thompson fracture fluids under most close to in situ salinity conditions (Figure 3). The overall $^{13}$C-depletion in DIC, with $\delta^{13}$C values in fracture water samples mostly below −20‰ (Table 3) further points to active microbial processes involving degradation of $^{13}$C-depleted organic carbon (cf., Claypool & Kaplan, 1974). The general dominance of heterotrophic metabolisms is similar to the high proportion of heterotrophic microorganisms identified in some of the Fennoscandian deep bedrock environments. At Outokumpu site, Finland, enrichment, genomic and metagenomic studies of subsurface microbial communities from various depths revealed high abundance of heterotrophic microorganisms capable of fermentation and oxidation of organic carbon (Nuppunen-Puputti et al., 2022; Nyyssönen et al., 2014; Purkamo et al., 2015). At these sites, ancient organic carbon from the bedrock or introduced to the subsurface due to later geotectonic events, are suggested as the carbon source for heterotrophic microorganisms (Drake et al., 2021; Purkamo et al., 2015).

At Thompson, the DOC concentrations are high compared to values previously reported in subsurface fracture fluids at various sites on the Fennoscandian Shield (e.g., Osterholz et al., 2022), and South Africa (e.g., Kieft et al., 2018). A similarly high DOC as FW#1 and #2 in this study (10.8–38.6 mM) was recently reported in deep brines from Moab Khotsong mine of the Witwatersrand Basin, South Africa (~8.5–23.6 mM; Nisson, Kieft, et al., 2023). Organic matter reworked by the effects of radiolysis is proposed as the primary source of the DOC in Moab Khotsong brines (Nisson,

Walters, et al., 2023). In that study, DOC composition analysis in fluids from a shallower depth (1.2 km) revealed, by comparison to deeper and older fluids, greater abundance of larger and more oxidized compounds, which had lower salinity and much higher cell abundance ($10^7$ cells $mL^{-1}$), indicating higher heterotrophic utilization (Nisson, Walters, et al., 2023). Possible sources of dissolved organic carbon in the deep subsurface include the Proterozoic metasedimentary rocks which are rich in organic carbon (Strauss, 1986), as proposed by Sherwood Lollar et al. (2021); surface-derived organic matter from recharge of paleometeoric water as identified in subsurface sites at the Fennoscandian Shield (Osterholz et al., 2022); or as suggested for the subsurface fluids of South Africa, mixtures of microbial necromass and metabolic products (Kieft et al., 2018), and organic matter reworked by the effects of radiolysis (Nisson, Walters, et al., 2023). The similarity of the $\delta^{13}C$ value of DOC for the adjacent Birchtree mine (−23.6‰ to −34.3‰) to that of organic carbon in the surrounding host rocks suggests that regardless of the specific processes involved, the ultimate origin of dissolved organic carbon in the fluids at Thompson is most likely derived from the host rocks (Sherwood Lollar et al., 2021).

### 4.2 | Impact of hydrogeological conditions on subsurface life at Thompson

Compared to subsurface saline fracture waters that are hydrogeologically isolated, there is generally higher biomass and diverse microbial groups in subsurface settings influenced by mixing with paleometeoric water, which are actively involved in deep cycles of C, S, and N. For example, in the 2.5-km-deep Outokumpu site, Finland, a relationship was observed with diverse archaeal and bacterial communities and depth, with cell densities decreasing from $10^5$ to $10^3$ cells $mL^{-1}$ over the depth profile, principally attributed to geological and hydrogeological conditions (Kietäväinen et al., 2013; Nyyssönen et al., 2014). Similarly, unlike the so-called "single-species ecosystem" dominated by chemoautotrophic $H_2$-utilizing sulfate reducers found in the South African gold mine Mponeng (Chivian et al., 2008; Lin et al., 2006), contributions of microbial methanogens and total overall biomass increased substantially in samples with higher degrees of paleometeoric water components at several subsurface sites in the Witwatersrand Basin, South Africa (Sherwood Lollar et al., 2006; Ward et al., 2004). At one site where mixing of older fracture water and paleometeoric waters has been identified (Simkus et al., 2016; Ward et al., 2004; Warr, Giunta, et al., 2021), highly diverse microbial communities including methanotrophs, $H_2$-utilizing methanogens and sulfate reducers, and sulfur-oxidizing denitrifiers were found to have developed metabolic symbiotic relationships to overcome oligotrophic conditions of the subsurface environments (Lau et al., 2016). Moreover, at this location, sulfur-driven denitrification is also found to dominate over $H_2$-driven sulfate-reducing metabolisms that had been emphasized in previous studies (Chivian et al., 2008; Lin et al., 2006).

Even within the three samples FW#3, #4 and #5 that are unimpacted by DW contamination, the most saline sample (FW#5) showed the lowest metabolic diversity and biomass ($10^3$ cells $mL^{-1}$) compared to FW#3 and #4. Within those 3 samples, an increase in total biomass, total MPNs and potential metabolic diversity was observed in FW#3. Both FW#3 and #4 have been more impacted by mixing with paleometeoric water than FW#5 based on their lower position on the mixing line (Figure 2a). This enhanced microbial activity observed here in paleometeoric water influenced FWs may suggest adaptive components of indigenous communities in deep fracture networks, which may be able to occupy a greater metabolic capacity when introduced to fresher (less saline) waters bearing additional energy and nutrient source (e.g., Mehrshad et al., 2021; Osterholz et al., 2022; Sherwood Lollar et al., 2007). Such a process can occur naturally by propagation of fractures in response to tectonic activity or episodic events (e.g., impacts, glacial rebound and uplift; Drake et al., 2021; Warr et al., 2019, 2022). Even in tectonically quiescent ancient shield rock such as at Thompson, modeling has shown that steady state deformation of the crust can sustain habitability through such fracture opening mechanisms (Sleep & Zoback, 2007). Collectively, the results from this study add new evidence to indicate that in the event of mixing between subsurface brine and fresher groundwater, subsurface microbial community structure can be significantly impacted (Sherwood Lollar et al., 2007).

## 5 | CONCLUSION

By applying the MPN-based approach, this study has investigated a series of different metabolic activity responses for subsurface microorganisms residing in the kilometer deep fracture waters of the Paleoproterozoic bedrocks at Thompson on the Canadian Shield. The results show extant microbial communities, some likely impacted by drilling fluids, while the more saline samples preserve what is likely to be an indigenous community of heterotrophic microbial groups fueled by high abundances of dissolved organic carbon. Specifically, the aerobic/facultative anaerobic heterotrophs, heterotrophic sulfate reducers, and general fermenters are among the most important components of the ecosystem. The most saline sample showed the lowest metabolic diversity and biomass ($10^3$ cells $mL^{-1}$) in line with observations elsewhere for the deep terrestrial subsurface biosphere, whereas other samples with decreasing salinities showed higher biomass and greater metabolic diversity. Results also show that decreased salinity may on one hand inhibit growth of low-biomass and low-diversity halophilic microorganisms, but on the other hand could trigger activity and biomass of highly diverse and less halotolerant microorganisms. In the context of natural systems, cycles of opening and closing of fracture networks over geological timescales can serve as a mechanism allowing mixing of deep saline fluids with fresher waters, potentially carrying additional energy sources or even surface organisms. As observed in this study, the effects of this long-term and large-scale mixing would similarly

significantly alter the subsurface microbial community structure and activity. Specifically, these results reveal that periodic cycling of local fractures may provide (and sustain) additional and hitherto unrecognized enhanced habitable zones in otherwise isolated and oligotrophic systems, where adaptive microbial communities may thrive. By exploring and characterizing these biological oases of the subsurface sites like this will provide additional insight on exploration of habitable zones both in Earth's deep subsurface and beyond, where hydrogeological conditions are one of the key factors to consider.

## ACKNOWLEDGMENTS

This study was financially supported by the Natural Sciences and Engineering Research Council of Canada Discovery and Accelerator grants (B.S.L) and Nuclear Waste Management Organization of Canada grants (B.S.L) with additional funding by CIFAR to Earth 4D Fellow B.S.L. We are grateful to the mine staff in Thompson mine for providing access to the sampling location. We thank Kenneth Voglesonger, James Moran, and Steffi Tille for collecting samples and for part of the geochemical analyses.

## CONFLICT OF INTEREST STATEMENT

The authors state no conflict of interest.

## DATA AVAILABILITY STATEMENT

The data generated in this study are provided in Appendix S1.

## ORCID

*Min Song* https://orcid.org/0000-0002-3291-0282
*Barbara Sherwood Lollar* https://orcid.org/0000-0001-9758-7095

## REFERENCES

Blodgett, R. (2010). *BAM appendix 2: Most probable number from serial dilutions. Bacteriological analytical manual*. Food and Drug Administration. https://www.fda.gov/food/foodscienceresearch/laboratorymethods/ucm109656.htm

Bomberg, M., Miettinen, H., Kietäväinen, R., Purkamo, L., Ahonen, L., & Vikman, M. (2021). Chapter 3 – Microbial metabolic potential in deep crystalline bedrock. In J. R. Lloyd & A. Cherkouk (Eds.), *The microbiology of nuclear waste disposal* (pp. 41–70). Elsevier.

Borgonie, G., García-Moyano, A., Litthauer, D., Bert, W., Bester, A., van Heerden, E., Möller, C., Erasmus, M., & Onstott, T. C. (2011). Nematoda from the terrestrial deep subsurface of South Africa. *Nature*, *474*(7349), 79–82.

Borgonie, G., Linage-Alvarez, B., Ojo, A. O., Mundle, S. O., Freese, L. B., Van Rooyen, C., Kuloyo, O., Albertyn, J., Pohl, C., & Cason, E. D. (2015). Eukaryotic opportunists dominate the deep-subsurface biosphere in South Africa. *Nature Communications*, *6*(1), 1–12.

Borgonie, G., Magnabosco, C., García-Moyano, A., Linage-Alvarez, B., Ojo, A. O., Freese, L. B., Van Jaarsveld, C., Van Rooyen, C., Kuloyo, O., & Cason, E. D. (2019). New ecosystems in the deep subsurface follow the flow of water driven by geological activity. *Scientific Reports*, *9*(1), 1–16.

Borton, M. A., Hoyt, D. W., Roux, S., Daly, R. A., Welch, S. A., Nicora, C. D., Purvine, S., Eder, E. K., Hanson, A. J., & Sheets, J. M. (2018). Coupled laboratory and field investigations resolve microbial interactions that underpin persistence in hydraulically fractured shales. *Proceedings of the National Academy of Sciences of the United States of America*, *115*(28), E6585–E6594.

Chi Fru, E. (2008). Constraints in the colonization of natural and engineered subterranean igneous rock aquifers by aerobic methane-oxidizing bacteria inferred by culture analysis. *Geobiology*, *6*(4), 365–375. https://doi.org/10.1111/j.1472-4669.2008.00164.x

Chivian, D., Brodie, E. L., Alm, E. J., Culley, D. E., Dehal, P. S., DeSantis, T. Z., Gihring, T. M., Lapidus, A., Lin, L.-H., & Lowry, S. R. (2008). Environmental genomics reveals a single-species ecosystem deep within Earth. *Science*, *322*(5899), 275–278.

Claypool, G. E., & Kaplan, I. (1974). The origin and distribution of methane in marine sediments. In *Natural gases in marine sediments* (pp. 99–139). Springer.

Coleman, M. L., Shepherd, T. J., Durham, J. J., Rouse, J. E., & Moore, G. R. (1982). Reduction of water with zinc for hydrogen isotope analysis. *Analytical Chemistry*, *54*(6), 993–995.

Cragg, B. A. (1994). Bacterial profiles in deep sediment layers from the Lau Basin, site 834. *Proceedings of the Ocean Drilling Program: Scientific Results*, *135*, 147–150.

Craig, H. (1961). Isotopic variations in meteoric waters. *Science*, *133*(3465), 1702–1703.

Daly, R. A., Borton, M. A., Wilkins, M. J., Hoyt, D. W., Kountz, D. J., Wolfe, R. A., Welch, S. A., Marcus, D. N., Trexler, R. V., & MacRae, J. D. (2016). Microbial metabolisms in a 2.5-km-deep ecosystem created by hydraulic fracturing in shales. *Nature Microbiology*, *1*(10), 1–9.

Doig, F., Sherwood Lollar, B., & Ferris, F. G. (1995). Microbial communities in deep Canadian shield groundwaters—An in situ biofilm experiment. *Geomicrobiology Journal*, *13*(2), 91–102. https://doi.org/10.1080/01490459509378008

Drake, H., Roberts, N. M. W., Reinhardt, M., Whitehouse, M., Ivarsson, M., Karlsson, A., Kooijman, E., & Kielman-Schmitt, M. (2021). Biosignatures of ancient microbial life are present across the igneous crust of the Fennoscandian shield. *Communications Earth & Environment*, *2*(1), 102. https://doi.org/10.1038/s43247-021-00170-2

Epstein, S., & Mayeda, T. (1953). Variation of O18 content of waters from natural sources. *Geochimica et Cosmochimica Acta*, *4*(5), 213–224.

Erkmen, O. (2022). Practice 4 - Most probable number technique. In O. Erkmen (Ed.), *Microbiological analysis of foods and food processing environments* (pp. 31–37). Academic Press. https://doi.org/10.1016/B978-0-323-91651-6.00042-2

Ferguson, G., McIntosh, J. C., Warr, O., Sherwood Lollar, B., Ballentine, C. J., Famiglietti, J. S., Kim, J. H., Michalski, J., Mustard, J. F., & Tarnas, J. (2021). Crustal groundwater volumes greater than previously thought. *Geophysical Research Letters*, *48*, e2021GL093549. https://doi.org/10.1029/2021GL093549

Frape, S. K., Blyth, A., Stotler, R. L., Ruskeeniemi, T., Blomqvist, R., McNutt, R. H., & Gascoyne, M. (2014). 7.15 – Deep fluids in the continents. In H. D. Holland & K. K. Turekian (Eds.), *Treatise on geochemistry* (2nd ed., pp. 517–562). Elsevier. https://doi.org/10.1016/B978-0-08-095975-7.00517-9

Frape, S. K., Fritz, P., & McNutt, R. H. (1984). Water-rock interaction and chemistry of groundwaters from the Canadian shield. *Geochimica et Cosmochimica Acta*, *48*(8), 1617–1627.

Gibson, J. J., Eby, P., Stadnyk, T. A., Holmes, T., Birks, S. J., & Pietroniro, A. (2021). Dataset of 18O and 2H in streamflow across Canada: A national resource for tracing water sources, water balance and predictive modelling. *Data in Brief*, *34*, 106723. https://doi.org/10.1016/j.dib.2021.106723

Goodwin, A. M. (1996). Chapter 1 – Distribution and tectonic setting of Precambrian crust. In A. M. Goodwin (Ed.), *Principles of Precambrian geology* (pp. 1–50). Academic Press. https://doi.org/10.1016/B978-012289770-2/50001-7

Grieve, R., & Therriault, A. (2000). Vredefort, Sudbury, Chicxulub: Three of a kind? *Annual Review of Earth and Planetary Sciences*, *28*, 305–338.

He, H., Wu, X., Xian, H., Zhu, J., Yang, Y., Lv, Y., Li, Y., & Konhauser, K. O. (2021). An abiotic source of Archean hydrogen peroxide and oxygen that pre-dates oxygenic photosynthesis. *Nature Communications*, *12*(1), 6611. https://doi.org/10.1038/s41467-021-26916-2

He, H., Wu, X., Zhu, J., Lin, M., Lv, Y., Xian, H., Yang, Y., Lin, X., Li, S., Li, Y., Teng, H. H., & Thiemens, M. H. (2023). A mineral-based origin of Earth's initial hydrogen peroxide and molecular oxygen. *Proceedings of the National Academy of Sciences of the United States of America*, *120*(13), e2221984120. https://doi.org/10.1073/pnas.2221984120

Heard, A. W., Warr, O., Borgonie, G., Linage, B., Kuloyo, O., Fellowes, J. W., Magnabosco, C., Lau, M. C., Erasmus, M., & Cason, E. D. (2018). South African crustal fracture fluids preserve paleometeoric water signatures for up to tens of millions of years. *Chemical Geology*, *493*, 379–395.

Holland, G., Sherwood Lollar, B., Li, L., Lacrampe-Couloume, G., Slater, G. F., & Ballentine, C. J. (2013). Deep fracture fluids isolated in the crust since the Precambrian era. *Nature*, *497*(7449), 357–360.

Hubalek, V., Wu, X., Eiler, A., Buck, M., Heim, C., Dopson, M., Bertilsson, S., & Ionescu, D. (2016). Connectivity to the surface determines diversity patterns in subsurface aquifers of the Fennoscandian shield. *The ISME Journal*, *10*(10), 2447–2458. https://doi.org/10.1038/ismej.2016.36

Hurley, M. A., & Roscoe, M. E. (1983). Automated statistical analysis of microbial enumeration by dilution series. *Journal of Applied Bacteriology*, *55*(1), 159–164.

Kadnikov, V. V., Mardanov, A. V., Beletsky, A. V., Karnachuk, O. V., & Ravin, N. V. (2020). Microbial life in the deep subsurface aquifer illuminated by metagenomics. *Frontiers in Microbiology*, *11*, 572252. https://doi.org/10.3389/fmicb.2020.572252

Kieft, T. L., Walters, C. C., Higgins, M. B., Mennito, A. S., Clewett, C. F., Heuer, V., Pullin, M. J., Hendrickson, S., van Heerden, E., & Sherwood Lollar, B. (2018). Dissolved organic matter compositions in 0.6–3.4 km deep fracture waters, Kaapvaal Craton, South Africa. *Organic Geochemistry*, *118*, 116–131.

Kietäväinen, R., Ahonen, L., Kukkonen, I. T., Hendriksson, N., Nyyssönen, M., & Itävaara, M. (2013). Characterisation and isotopic evolution of saline waters of the Outokumpu deep drill hole, Finland – Implications for water origin and deep terrestrial biosphere. *Applied Geochemistry*, *32*, 37–51. https://doi.org/10.1016/j.apgeochem.2012.10.013

Kietäväinen, R., Ahonen, L., Kukkonen, I. T., Niedermann, S., & Wiersberg, T. (2014). Noble gas residence times of saline waters within crystalline bedrock, Outokumpu Deep Drill Hole, Finland. *Geochimica et Cosmochimica Acta*, *145*, 159–174.

Kraft, B., Jehmlich, N., Larsen, M., Bristow, L. A., Könneke, M., Thamdrup, B., & Canfield, D. E. (2022). Oxygen and nitrogen production by an ammonia-oxidizing archaeon. *Science*, *375*(6576), 97–100. https://doi.org/10.1126/science.abe6733

Lau, M. C., Kieft, T. L., Kuloyo, O., Linage-Alvarez, B., Van Heerden, E., Lindsay, M. R., Magnabosco, C., Wang, W., Wiggins, J. B., & Guo, L. (2016). An oligotrophic deep-subsurface community dependent on syntrophy is dominated by sulfur-driven autotrophic denitrifiers. *Proceedings of the National Academy of Sciences of the United States of America*, *113*(49), E7927–E7936.

Li, L., Wei, S., Sherwood Lollar, B., Wing, B., Bui, T. H., Ono, S., Lau Vetter, M. C. Y., Onstott, T. C., Kieft, T. L., Borgonie, G., Linage-Alvarez, B., Kuloyo, O., & van Heerden, E. (2022). In situ oxidation of sulfide minerals supports widespread sulfate reducing bacteria in the deep subsurface of the Witwatersrand Basin (South Africa): Insights from multiple sulfur and oxygen isotopes. *Earth and Planetary Science Letters*, *577*, 117247. https://doi.org/10.1016/j.epsl.2021.117247

Li, L., Wing, B., Bui, T., McDermott, J., Slater, G., Wei, S., Lacrampe-Couloume, G., & Sherwood Lollar, B. (2016). Sulfur mass-independent fractionation in subsurface fracture waters indicates a long-standing sulfur cycle in Precambrian rocks. *Nature Communications*, *7*(1), 1–9.

Lightfoot, P. C., Stewart, R., Gribbin, G., & Mooney, S. J. (2017). Relative contribution of magmatic and post-magmatic processes in the genesis of the Thompson mine Ni-Co sulfide ores, Manitoba, Canada. *Ore Geology Reviews*, *83*, 258–286.

Lin, L. H., Hall, J., Lippmann-Pipke, J., Ward, J. A., Sherwood Lollar, B., DeFlaun, M., Rothmel, R., Moser, D., Gihring, T. M., & Mislowack, B. (2005). Radiolytic H2 in continental crust: Nuclear power for deep subsurface microbial communities. *Geochemistry, Geophysics, Geosystems*, *6*(7), Q07003. https://doi.org/10.1029/2004GC000907

Lin, L.-H., Slater, G. F., Lollar, B. S., Lacrampe-Couloume, G., & Onstott, T. C. (2005). The yield and isotopic composition of radiolytic H2, a potential energy source for the deep subsurface biosphere. *Geochimica et Cosmochimica Acta*, *69*(4), 893–903.

Lin, L.-H., Wang, P.-L., Rumble, D., Lippmann-Pipke, J., Boice, E., Pratt, L. M., Sherwood Lollar, B., Brodie, E. L., Hazen, T. C., & Andersen, G. L. (2006). Long-term sustainability of a high-energy, low-diversity crustal biome. *Science*, *314*(5798), 479–482.

Lippmann, J., Stute, M., Torgersen, T., Moser, D., Hall, J., Lin, L., Borcsik, M., Bellamy, R., & Onstott, T. C. (2003). Dating ultra-deep mine waters with noble gases and 36Cl, Witwatersrand Basin, South Africa. *Geochimica et Cosmochimica Acta*, *67*(23), 4597–4619.

Lollar, G. S., Warr, O., Telling, J., Osburn, M. R., & Sherwood Lollar, B. (2019). 'Follow the water': Hydrogeochemical constraints on microbial investigations 2.4 km below surface at the kidd creek deep fluid and deep life observatory. *Geomicrobiology Journal*, *36*(10), 859–872.

Lovley, D. R., & Chapelle, F. H. (1995). Deep subsurface microbial processes. *Reviews of Geophysics*, *33*(3), 365–381.

Magnabosco, C., Lin, L.-H., Dong, H., Bomberg, M., Ghiorse, W., Stan-Lotter, H., Pedersen, K., Kieft, T., Van Heerden, E., & Onstott, T. C. (2018). The biomass and biodiversity of the continental subsurface. *Nature Geoscience*, *11*(10), 707–717.

Magnabosco, C., Ryan, K., Lau, M. C., Kuloyo, O., Lollar, B. S., Kieft, T. L., Van HeerDen, E., & Onstott, T. C. (2016). A metagenomic window into carbon metabolism at 3 km depth in Precambrian continental crust. *The ISME Journal*, *10*(3), 730–741.

Mehrshad, M., Lopez-Fernandez, M., Sundh, J., Bell, E., Simone, D., Buck, M., Bernier-Latmani, R., Bertilsson, S., & Dopson, M. (2021). Energy efficiency and biological interactions define the core microbiome of deep oligotrophic groundwater. *Nature Communications*, *12*(1), 1–12.

National Academies of Sciences, E., and Medicine. (2022). *Origins, worlds, and life: A decadal strategy for planetary science and astrobiology 2023–2032*. The National Academies Press. https://doi.org/10.17226/26522

Nisson, D., Kieft, T., Drake, H., Warr, O., Sherwood Lollar, B., Ogasawara, H., Perl, S., Friefeld, B., Castillo, J., & Whitehouse, M. J. (2023). Hydrogeochemical and isotopic signatures elucidate deep subsurface hypersaline brine formation through radiolysis driven water-rock interaction. *Geochimica et Cosmochimica Acta*, *340*, 65–84.

Nisson, D. M., Walters, C. C., Chacón-Patiño, M. L., Weisbrod, C. R., Kieft, T. L., Sherwood Lollar, B., Warr, O., Castillo, J., Perl, S. M., Cason, E. D., Freifeld, B. M., & Onstott, T. C. (2023). Radiolytically reworked Archean organic matter in a habitable deep ancient high-temperature brine. *Nature Communications*, *14*(1), 6163. https://doi.org/10.1038/s41467-023-41900-8

Nuppunen-Puputti, M., Kietäväinen, R., Raulio, M., Soro, A., Purkamo, L., Kukkonen, I., & Bomberg, M. (2022). Epilithic microbial community functionality in deep oligotrophic continental bedrock. *Frontiers in Microbiology*, *13*, 826048. https://doi.org/10.3389/fmicb.2022.826048

Nyyssönen, M., Hultman, J., Ahonen, L., Kukkonen, I., Paulin, L., Laine, P., Itävaara, M., & Auvinen, P. (2014). Taxonomically and functionally diverse microbial communities in deep crystalline rocks of the Fennoscandian shield. *The ISME Journal*, *8*(1), 126–138.

Oblinger, J., & Koburger, J. (1975). Understanding and teaching the most probable number technique. *Journal of Milk and Food Technology*, *38*(9), 540–545.

Onstott, T. C., Ehlmann, B. L., Sapers, H., Coleman, M., Ivarsson, M., Marlow, J. J., Neubeck, A., & Niles, P. (2019). Paleo-rock-hosted life on Earth and the search on Mars: A review and strategy for exploration. *Astrobiology*, *19*(10), 1230–1262.

Onstott, T. C., Lin, L.-H., Davidson, M., Mislowack, B., Borcsik, M., Hall, J., Slater, G., Ward, J., Sherwood Lollar, B., & Lippmann-Pipke, J. (2006). The origin and age of biogeochemical trends in deep fracture water of the Witwatersrand Basin, South Africa. *Geomicrobiology Journal*, *23*(6), 369–414.

Oremland, R. S., & Des Marais, D. J. (1983). Distribution, abundance and carbon isotopic composition of gaseous hydrocarbons in Big Soda Lake, Nevada: An alkaline, meromictic lake. *Geochimica et Cosmochimica Acta*, *47*(12), 2107–2114.

Osterholz, H., Turner, S., Alakangas, L. J., Tullborg, E.-L., Dittmar, T., Kalinowski, B. E., & Dopson, M. (2022). Terrigenous dissolved organic matter persists in the energy-limited deep groundwaters of the Fennoscandian Shield. *Nature Communications*, *13*(1), 4837. https://doi.org/10.1038/s41467-022-32457-z

Paventi, M. (1995). *Rock mass characteristics and damage at the Birchtree Mine*. [Doctoral dissertation, McGill University, Quebec, Canada].

Pedersen, K., Bengtsson, A. F., Edlund, J. S., & Eriksson, L. C. (2014). Sulphate-controlled diversity of subterranean microbial communities over depth in deep groundwater with opposing gradients of sulphate and methane. *Geomicrobiology Journal*, *31*(7), 617–631.

Purkamo, L., Bomberg, M., Kietäväinen, R., Salavirta, H., Nyyssönen, M., Nuppunen-Puputti, M., Ahonen, L., Kukkonen, I., & Itävaara, M. (2016). Microbial co-occurrence patterns in deep Precambrian bedrock fracture fluids. *Biogeosciences*, *13*(10), 3091–3108.

Purkamo, L., Bomberg, M., Nyyssönen, M., Kukkonen, I., Ahonen, L., & Itävaara, M. (2015). Heterotrophic communities supplied by ancient organic carbon predominate in deep Fennoscandian bedrock fluids. *Microbial Ecology*, *69*(2), 319–332.

Ruff, S. E., Humez, P., de Angelis, I. H., Diao, M., Nightingale, M., Cho, S., Connors, L., Kuloyo, O. O., Seltzer, A., & Bowman, S. (2023). Hydrogen and dark oxygen drive microbial productivity in diverse groundwater ecosystems. *Nature Communications*, *14*(1), 3194.

Sauvage, J. F., Flinders, A., Spivack, A. J., Pockalny, R., Dunlea, A. G., Anderson, C. H., Smith, D. C., Murray, R. W., & D'Hondt, S. (2021). The contribution of water radiolysis to marine sedimentary life. *Nature Communications*, *12*(1), 1–9.

Sheik, C., Badalamenti, J., Telling, J., Hsu, D., Alexander, S. C., Bond, D. R., Gralnick, J. A., Sherwood Lollar, B., & Toner, B. M. (2021). Novel microbial groups drive productivity in an Archean iron formation. *Frontiers in Microbiology*, *12*, 616.

Sheik, C. S., Reese, B. K., Twing, K. I., Sylvan, J. B., Grim, S. L., Schrenk, M. O., Sogin, M. L., & Colwell, F. S. (2018). Identification and removal of contaminant sequences from ribosomal gene databases: Lessons from the census of deep life. *Frontiers in Microbiology*, *9*, 840.

Sherwood Lollar, B., Frape, S. K., Fritz, P., Macko, S. A., Welhan, J. A., Blomqvist, R., & Lahermo, P. W. (1993). Evidence for bacterially generated hydrocarbon gas in Canadian shield and Fennoscandian shield rocks. *Geochimica et Cosmochimica Acta*, *57*(23), 5073–5085.

Sherwood Lollar, B., Heuer, V. B., McDermott, J., Tille, S., Warr, O., Moran, J., Telling, J., & Hinrichs, K.-U. (2021). A window into the abiotic carbon cycle–acetate and formate in fracture waters in 2.7 billion year-old host rocks of the Canadian Shield. *Geochimica et Cosmochimica Acta*, *294*, 295–314.

Sherwood Lollar, B., Lacrampe-Couloume, G., Slater, G., Ward, J., Moser, D. P., Gihring, T., Lin, L.-H., & Onstott, T. C. (2006). Unravelling abiogenic and biogenic sources of methane in the Earth's deep subsurface. *Chemical Geology*, *226*(3–4), 328–339.

Sherwood Lollar, B., Onstott, T. C., Lacrampe-Couloume, G., & Ballentine, C. (2014). The contribution of the Precambrian continental lithosphere to global $H_2$ production. *Nature*, *516*(7531), 379–382.

Sherwood Lollar, B., Voglesonger, K., Lin, L.-H., Lacrampe-Couloume, G., Telling, J., Abrajano, T., Onstott, T. C., & Pratt, L. (2007). Hydrogeologic controls on episodic H2 release from Precambrian fractured rocks—Energy for deep subsurface life on Earth and Mars. *Astrobiology*, *7*(6), 971–986.

Sherwood Lollar, B., Westgate, T., Ward, J., Slater, G., & Lacrampe-Couloume, G. (2002). Abiogenic formation of alkanes in the Earth's crust as a minor source for global hydrocarbon reservoirs. *Nature*, *416*(6880), 522–524.

Simkus, D. N., Slater, G. F., Sherwood Lollar, B., Wilkie, K., Kieft, T. L., Magnabosco, C., Lau, M. C., Pullin, M. J., Hendrickson, S. B., & Wommack, K. E. (2016). Variations in microbial carbon sources and cycling in the deep continental subsurface. *Geochimica et Cosmochimica Acta*, *173*, 264–283.

Sleep, N. H., & Zoback, M. D. (2007). Did earthquakes keep the early crust habitable? *Astrobiology*, *7*(6), 1023–1032.

Standard Methods Committee of the American Public Health Association American Water Works Association and Water Environment Federation. (2018). 4500-NH3 nitrogen (ammonia). In B. T. Lipps & E. Braun-Howland (Eds.), *Standard methods for the examination of water and wastewater*. APHA Press. https://doi.org/10.2105/smww.2882.087

Stone, J., Edgar, J. O., Gould, J. A., & Telling, J. (2022). Tectonically-driven oxidant production in the hot biosphere. *Nature Communications*, *13*(1), 4529.

Stookey, L. L. (1970). Ferrozine – A new spectrophotometric reagent for iron. *Analytical Chemistry*, *42*(7), 779–781.

Strauss, H. (1986). Carbon and sulfur isotopes in Precambrian sediments from the Canadian Shield. *Geochimica et Cosmochimica Acta*, *50*(12), 2653–2662.

Telling, J., Voglesonger, K., Sutcliffe, C. N., Lacrampe-Couloume, G., Edwards, E., & Sherwood Lollar, B. (2018). Bioenergetic constraints on microbial hydrogen utilization in Precambrian deep crustal fracture fluids. *Geomicrobiology Journal*, *35*(2), 108–119.

Trembath-Reichert, E., Shah Walter, S. R., Ortiz, M. A. F., Carter, P. D., Girguis, P. R., & Huber, J. A. (2021). Multiple carbon incorporation strategies support microbial survival in cold subseafloor crustal fluids. *Science Advances*, *7*(18), eabg0153. https://doi.org/10.1126/sciadv.abg0153

Ward, J. A., Slater, G. F., Moser, D. P., Lin, L. H., Lacrampe-Couloume, G., Bonin, A. S., Davidson, M., Hall, J. A., Mislowack, B., Bellamy, R. E. S., Onstott, T. C., & Sherwood Lollar, B. (2004). Microbial hydrocarbon gases in the Witwatersrand Basin, South Africa: Implications for the deep biosphere. *Geochimica et Cosmochimica Acta*, *68*(15), 3239–3250. https://doi.org/10.1016/j.gca.2004.02.020

Warr, O., Ballentine, C., Onstott, T., Nisson, D., Kieft, T., Hillegonds, D., & Sherwood Lollar, B. (2022). 86Kr excess and other noble gases identify a billion-year-old radiogenically-enriched groundwater system. *Nature Communications*, *13*, 3768.

Warr, O., Giunta, T., Ballentine, C. J., & Sherwood Lollar, B. (2019). Mechanisms and rates of 4He, 40Ar, and H2 production and accumulation in fracture fluids in Precambrian Shield environments. *Chemical Geology*, *530*, 119322.

Warr, O., Giunta, T., Onstott, T. C., Kieft, T. L., Harris, R. L., Nisson, D. M., & Sherwood Lollar, B. (2021). The role of low-temperature 18O exchange in the isotopic evolution of deep subsurface fluids. *Chemical Geology*, *561*, 120027.

Warr, O., Sherwood Lollar, B., Fellowes, J., Sutcliffe, C. N., McDermott, J. M., Holland, G., Mabry, J. C., & Ballentine, C. J. (2018). Tracing ancient hydrogeological fracture network age and compartmentalisation using noble gases. *Geochimica et Cosmochimica Acta*, *222*, 340–362.

Warr, O., Young, E. D., Giunta, T., Kohl, I. E., Ash, J. L., & Sherwood Lollar, B. (2021). High-resolution, long-term isotopic and isotopologue variation identifies the sources and sinks of methane in a deep subsurface carbon cycle. *Geochimica et Cosmochimica Acta*, *294*, 315–334.

Westmeijer, G., Mehrshad, M., Turner, S., Alakangas, L., Sachpazidou, V., Bunse, C., Pinhassi, J., Ketzer, M., Åström, M., Bertilsson, S., & Dopson, M. (2022). Connectivity of Fennoscandian Shield terrestrial deep biosphere microbiomes with surface communities. *Communications Biology*, *5*(1), 37. https://doi.org/10.1038/s42003-021-02980-8

Woodward, R. L. (1957). How probable is the most probable number? *Journal American Water Works Association*, *49*(8), 1060–1068.

Zwanzig, H., Macek, J., & McGregor, C. (2007). Lithostratigraphy and geochemistry of the high-grade metasedimentary rocks in the Thompson Nickel Belt and adjacent Kisseynew Domain, Manitoba: Implications for nickel exploration. *Economic Geology*, *102*(7), 1197–1216.

## SUPPORTING INFORMATION

Additional supporting information can be found online in the Supporting Information section at the end of this article.

**How to cite this article:** Song, M., Warr, O., Telling, J., & Sherwood Lollar, B. (2024). Hydrogeological controls on microbial activity and habitability in the Precambrian continental crust. *Geobiology*, *22*, e12592. https://doi.org/10.1111/gbi.12592